INL/EXT-16-38852 Rev1

VCTR: A Versatile Coupled Test Reactor Concept

G. Youinou, S. Sen, P. Henslee, M. Salvatores,

G. Palmiotti, R. Wigeland, D. Hill, C. Davis,

S. Pirmet*, S. Hayes, J. Bumgardner, P. Finck

May 2016

* 2016 summer intern from École Polytechnique de Paris, France

The INL is a U.S. Department of Energy National Laboratory
operated by Battelle Energy Alliance

Date of Revision 1: September 21, 2016

Purpose of Revision 1:

- Chapter 3 introduces the notion of boosted configurations which aim at minimizing core power and fissile inventory.
- Chapter 5 briefly mentions the German experimental reactor KNK whose experience is relevant to the present work and provides a reference for the interested reader.
- Chapter 8 has been divided into 2 sections. Section 8.1 contains the same material as the original Chapter 8. Section 8.2 contains additional information about other coupled configurations which aim at providing additional control of the irradiation conditions in the thermal region.
- Two more references have been added (5 and 16).

Table of Contents

Executive Summary ii

1. Introduction 1

2. What is a versatile test reactor? 3

3. What is a coupled test reactor? 4

4. Key design principles 6

5. Major options considered 6

6. Computer codes used for physics and thermal analyses 8

7. Neutronics analyses of an LEU configuration aiming at minimizing core power and fissile inventory 9

8. Neutronics analyses of Pu-LEU configurations 15

8.1 Configuration aiming at minimizing core power and plutonium inventory of the fast zone 15

8.2 Configuration aiming at providing additional control of the irradiation conditions in the thermal zone 16

9. Preliminary thermal analyses 20

10. Preliminary neutron kinetics analyses 25

11. Systems considerations 27

12. Safety considerations 34

13. Conclusions 37

14. References 38

Appendix A. Theory of coupled reactors 39

Appendix B. Notes on the physics of neutronics coupling 50

Appendix C. Preliminary coupled reactor deterministic calculations using MAMMOTH 53

Executive Summary

The United States has the facilities necessary to cover the need for thermal neutron irradiations, however, there is currently an important gap regarding fast neutron irradiations. In order to ensure the long term relevance of a new test reactor, the latter should be highly reconfigurable and allow operation as a fast test reactor or as a thermal test reactor or as a coupled fast-thermal test reactor in order to satisfy the needs, present and future, of as many customers as possible. In addition to the possibility to generate high fast and thermal neutron fluxes, the use of sodium as coolant in conjunction with a solid moderator such as graphite opens the door for such highly reconfigurable cores.

A distinction can be made depending on the main purpose of using fuel assemblies with some level of neutron moderation (thermal zone) together with fuel assemblies with as little moderation as possible (fast zone). It can be used mainly to minimize the core power and fissile inventory—in this case the configuration is said to be boosted—or it can be used mainly to provide additional control of the irradiation conditions in the thermal zone. The extent to which both objectives can be reached at the same time depends on other constraints such as the total power of the reactor.

One important finding presented in this report is that a boosted core configuration using only low enriched uranium fuel could provide both a high fast neutron flux and a high thermal neutron flux—respectively 3.5×10^{15} n/s.cm^2 and 10^{15} n/s.cm^2—in large volumes while at the same time maintaining core power below 300 MW. The use of plutonium in the fast zone would provide more flexibility in fuel assembly design than when low enriched uranium is used because, the reactivity worth of plutonium being higher than that of uranium-235, the designer has more degrees of freedom to work with; in particular it could provide additional control of the irradiation conditions in the thermal zone. A system level cost-benefit analysis regarding the use of plutonium vs. the use of only low enriched uranium will be necessary in the near future in order to make informed decision.

1. Introduction

In order to support the large number of US reactors it is important to have of a strong and dedicated research infrastructure to carry out the various tests necessary to improve performance, safety and validate potential new fuels and materials. Thermal neutron test reactors such as INL Advanced Test Reactor (ATR) currently provide most of the services required by the US civilian nuclear industry and by the US Navy plus other services such as isotope production. However, despite the vast recognized potential of fast neutron reactors for waste management, energy system sustainability and resources preservation in a low-carbon perspective, the United States has currently no domestic fast neutron test and irradiation capabilities necessary to pursue a strong research and development program related to fast neutron reactors. This lack prevents the testing of fast reactor fuels in a prototypic environment, the testing of new safety features and of new coolants. Potential vendors exploring different fast reactor concepts with technical support from DOE that need access to fast neutrons include: TerraPower (sodium or molten salts), General Atomics EM2 (gas), and Westinghouse LFR (lead). Given this broad range of technology options, a versatile test facility to enable a broad range of operating conditions, coolant types, and fuel designs is necessary. Several new facilities are presently under construction in the world, e.g. the JHR in France [1] and MBIR in Russia [2], each dedicated primarily to one type of spectrum; hence the unique features and potential offered by a coupled spectra reactor are of particular interest.

Figure 1.1. Start-up of the JHR reactor in Cadarache, France, is scheduled for 2019.

Figure 1.2. First concrete was poured at the construction site of the MBIR reactor in Dimitrovgrad, Russia, in September 2015. Start-up is scheduled for 2020.

In fact, whereas today the United States has the facilities necessary to cover the need for thermal neutron irradiation, there is currently an important gap regarding fast neutron irradiation. Furthermore, whether or not current thermal neutron irradiation facilities such as ATR will be able to fulfill future needs for thermal neutron irradiations is also an open question. For example the use of molten salt loop in ATR would be very difficult if not impossible. It is important we anticipate future thermal neutron irradiation needs.

A new irradiation test reactor is a costly investment that will operate for several decades and the initial specifications are crucial to ensure the relevance of such a facility in the long run. This new test reactor should be highly reconfigurable and allow operation as a fast test reactor or a thermal test reactor or a coupled fast-thermal test reactor. This report presents the on-going effort at Idaho National Laboratory (INL) to design a versatile coupled test reactor (VCTR) that could fulfill the R&D needs requiring high fast neutron fluxes but also high thermal neutron fluxes in configurations that could not be met in current thermal neutron test reactors such as ATR.

The objective of this report is to summarize the efforts undertaken at INL from May 2015 to March 2016 aimed at understanding the main options for designing and building a *versatile* test reactor, with a primary mission to provide thermal and fast neutrons for irradiation of fuels and materials in a manner complementary to the ATR and to the Oak Ridge National Laboratory (ORNL) High Flux Isotope Reactor (HFIR). Other missions can also be considered, including the validation of computer codes and the development of specific reactor technologies.

A domestic versatile neutron irradiation facility will be a critical tool to **enable rapid innovation** in the US: it will serve to do **performance testing** of new fuels and materials, and it will provide the data needed for **establishing a science based accelerating testing capability** that will give our industry a strong competitive advantage.

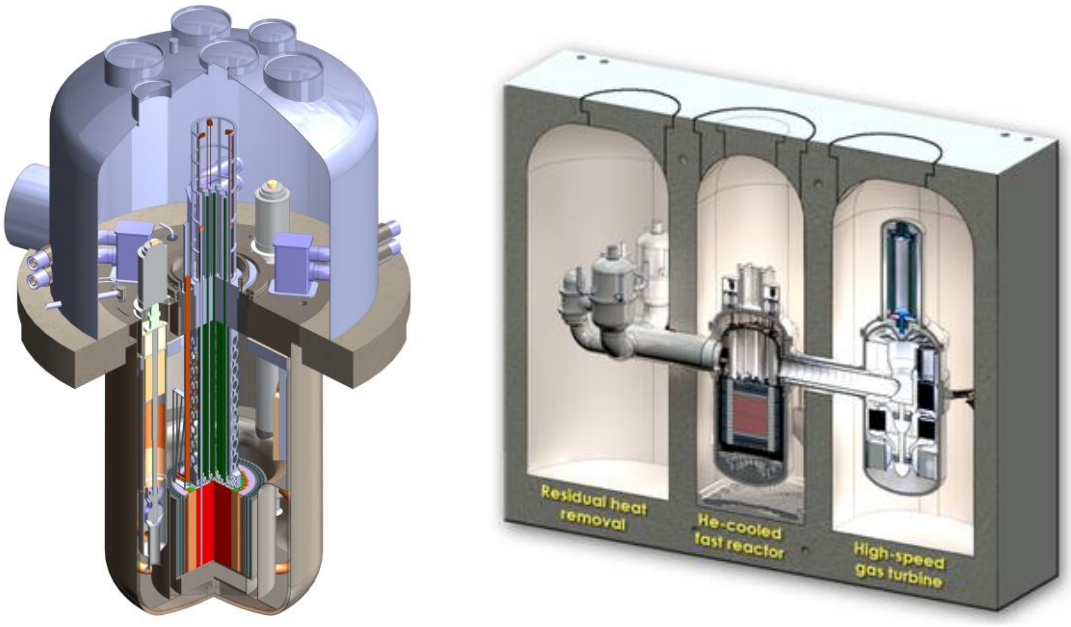

Figure 1.3. Innovative concepts such as developed by TerraPower (left) and General Atomics (EM2, right) would benefit from the availability of a domestic versatile neutron irradiation facility

2. What is a versatile test reactor?

The notion of versatility has been mentioned in various contexts, but has never been fully defined. While there is a desire in the research community to design a reactor that can accomplish multiple functions, there is also a good understanding within the reactor design community that a clear set of *prioritized* reactor functions needs to be defined a priori for allowing the design and operations of an efficient reactor.

This prioritized list must of course be developed as a function of potential user needs. There has been sufficient early work with DOE-NE to have a general understanding of these needs, even though further discussions with users will be needed to settle down clear priorities and specific requirements. In particular recent analyses indicate a significant gap in the US and potentially elsewhere for fast neutron irradiations; furthermore, the limits of existing thermal irradiation reactors in the US (ATR, HFIR) are well known, and a complementary capability would be useful.

These considerations provided the basic definition of a *versatile* test reactor used in this study:

- Function 1: this reactor will provide a fast flux irradiation environment prototypical of potential fast reactor designs:
    - The fast flux level will be equivalent to that of existing fast test reactors, i.e. at least 4×10^{15} n/cm^2.s
    - The irradiation volume will be sufficient to accommodate a volume equivalent to a fuel assembly
    - The irradiation environment should be flexible, and accommodate a number of potential reactor coolants.
    - A number of different irradiation vehicles will be allowed for: loops, instrumented assemblies, test samples, rabbits.
    - Experimental capabilities should enable both integral “traditional” testing, and science based testing

- Function 2: this reactor will provide thermal and epithermal flux irradiation environments complementary to those of ATR and HFIR:
    - The thermal flux level will be equivalent to that of ATR, i.e. at least 5×10^{14} n/cm^2.s
    - The irradiation volume will be equivalent to that of ATR
    - The irradiation environment should allow for irradiations that are not possible today in ATR and HFIR; this includes loops with various coolants

- Function 3: other possibilities, including beam tubes for scientific experiments, irradiation vehicles for isotope production, support for code validation, and support for reactor technology demonstration will need to be studied during the pre-conceptual design phase.

3. What is a coupled test reactor?

In this work, a coupled reactor is defined as a reactor with two distinct spectral zones (Fast and Thermal), which are neutronically coupled to each other; some neutrons born in zone F cause fission in zone T and vice-versa. Only fast neutrons are allowed to go from one zone to the other. A neutron filter keeps thermal neutrons from diffusing into the fast zone.

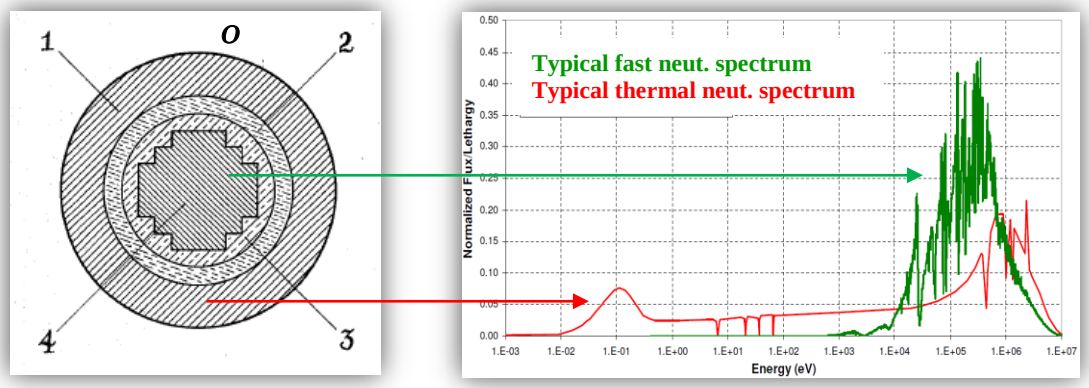

*Figure 3.1. Illustration of a coupled reactor (**0**- outer reflector; **1**- thermal annular core; **2**- inner reflector; **3**- thermal neutron filter; **4**- fast core)*

The idea of coupling a fast and a thermal zone is not new; the first US patent was filed in 1957 by R. Avery [3] and the theory he developed to describe a coupled reactor is presented in **Appendix A**. The objective of Avery's design was to benefit from the presence of fast neutrons to breed plutonium and at the same time benefit from the presence of thermal neutrons, which make the control of the reactor closer to that of a thermal reactor for which there was more experience. This was seen as the best of both worlds at the time. However, as time went by and experience increased, nuclear engineers became accustomed to the control of fast neutron reactors and the idea of a thermal-fast power reactor was abandoned. The idea was however adopted for zero-power facilities—STEK [4] for example, see Figure 3.2—used to do fast neutron physics measurements as well as, to some extent, for the 58 MWt experimental reactor KNK-II [5] built in Germany in the 70's.

A coupled core is characterized by the neutron multiplicity of each zone as well as by the coupling between the two zones. Four integral parameters are necessary to characterize the neutron physics of a fast-thermal coupled system

- ✓ k_F: average number of next generation neutrons in fast zone resulting from a single fission neutron in fast zone
- ✓ k_T: average number of next generation neutrons in thermal zone resulting from a single fission neutron in thermal zone
- ✓ k_{FT}: average number of next generation fission neutrons in thermal zone resulting from a single fission neutron in fast zone
- ✓ k_{TF}: average number of next generation fission neutrons in fast zone resulting from a single fission neutron in thermal zone

If the fast and thermal zones are sufficiently far apart, each zone needs to be critical by itself, i.e. the thermal-fast system is critical if $k_F = 1$ and $k_T = 1$. The two zones are decoupled ($k_{FT} = k_{TF} = 0$) and, from a neutronic point of view, equivalent to two separate reactors. On the other hand, if the system is designed such that the fast and thermal zones are neutronically coupled, then each zone taken individually is subcritical ($k_F < 1$ and $k_T < 1$) and, as demonstrated in Appendix A, the coupled system is critical only if the product of the coupling coefficients is equal to the product of the local subcriticalities (1-k), i.e.

$$k_{FT}k_{TF} = (1 - k_F)(1 - k_T)$$

In such a coupled critical system, the power in a given zone reacts to changes in the other zone; the ratio of the power in each zone is determined by the following expression:

$$\frac{P_F}{P_T} = \frac{k_{TF}}{1 - k_F} = \frac{1 - k_T}{k_{FT}}$$

From this expression it can be concluded that a coupled system will be less sensitive to uncertainties—or perturbations—occurring in the fissile zones if they are far from critical. For example, an uncertainty of 0.005 on the neutron multiplicity of the fast zone, k_F, corresponds to an uncertainty of about 2.5 percent on the ratio P_F over P_T if k_F = 0.8 and to uncertainty of about 10 percent on the same ratio if k_F = 0.95. Put differently, **the farther k_F and k_T are from 1 and the closer k_{FT} and k_{TF} are from 1, the more stable the system is**. This has important consequences on the operation and safety of the reactor and it should be kept in mind in the design process. A more detailed physics explanation is provided in **Appendix B.**

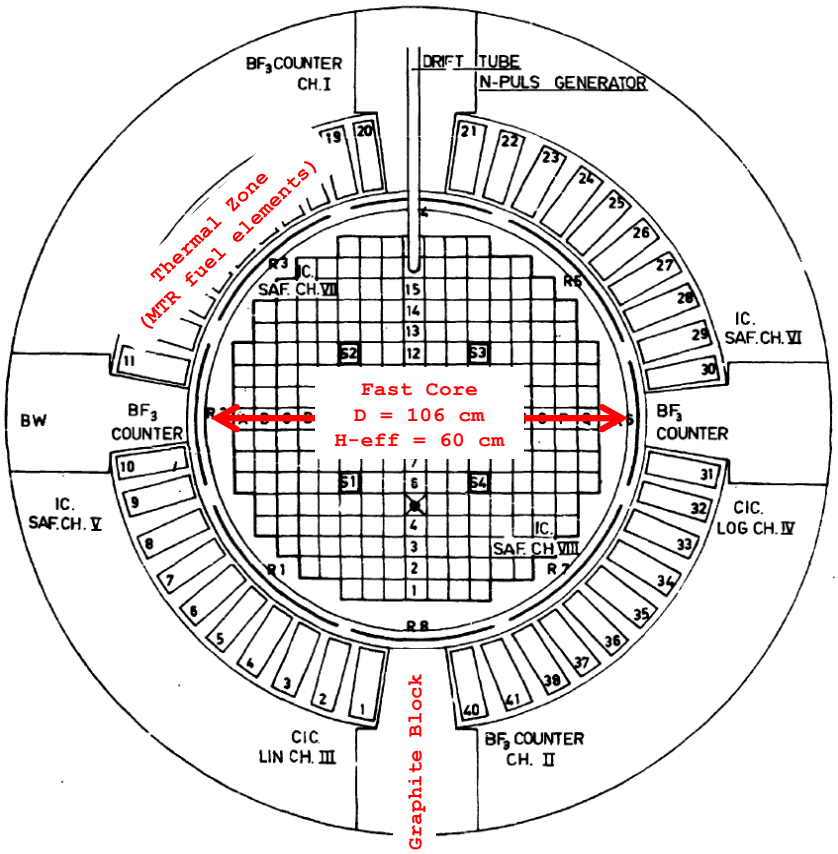

Figure 3.2. Coupled fast-thermal zero power facility STEK used to perform physics measurement at RCN Petten

A distinction can be made depending on the main purpose of using fuel assemblies with some level of neutron moderation (thermal zone) together with fuel assemblies with as little moderation as possible (fast zone). It can be used mainly to minimize the power and fissile inventory in the fast zone—by providing reactivity that would otherwise need to come from the fast zone—or it can be used mainly to provide additional control of the irradiation conditions in the thermal zone—by minimizing flux gradients for example. In the first case, the coupling coefficients, k_{FT} and k_{TF}, are maximized by bringing the moderated fuel assemblies as close to the fast zone as possible; the configuration is said to be **boosted**. In the second case, the impact on the power and fissile inventory of the fast zone will be less because the objective of the thermal fuel assemblies is to provide additional control of the irradiation conditions in the thermal zone; the

coupling coefficients will be smaller than in the first, boosted, case (Figure 3.3). The extent to which both objectives can be reached at the same time depends on other constraints such as the total power of the reactor.

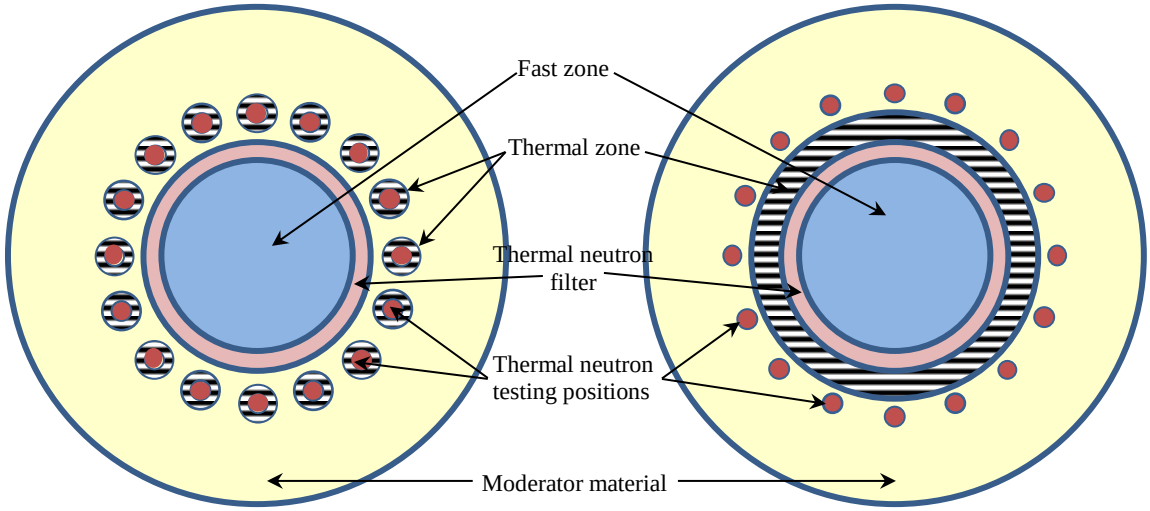

Figure 3.3. Illustration of two coupled configurations aiming at either providing additional control of irradiation conditions in the thermal zone (left) or minimizing the power and fissile inventory in the fast zone (right)

4. Key design principles

A number of considerations needed to be included in this early design effort; we focused on the key following principles:

- The reactor needs to be built rapidly, and with limited technological risk; thus, we decided to rely entirely on well demonstrated technologies.

- The reactor is first and foremost an irradiation machine; therefore all design choices must be made to enable and facilitate experimentation

- While it is desirable to have thermal, epithermal, and fast irradiation capabilities at the same time, various options should be considered where fast and thermal irradiations can be performed at separate times. This implies a flexible reconfigurable design.

- Specific performance objectives need to be decided with the user community. Nevertheless for this effort the objective is to reach fast and thermal flux levels at least equivalent to those of existing international test reactors

5. Major options considered in this study

Four key design challenges were identified at the onset of this study:

- Engineering feasibility led us to adopt designs with a single low-pressure coolant; in order to achieve high fast flux levels and remain within the realm of demonstrated technologies sodium is the preferred coolant choice.

- Engineering feasibility also led us to adopt the use of canned graphite as moderator. Beryllium, also a very good neutron moderator, was not considered because of the difficulties associated with its disposal.[1] However, a cost-benefit analysis regarding its use should be carried out in the near future. Zirconium hydride is also another potential neutron moderator candidate.

- Resources of fissile materials, safeguards issues, and used fuel disposition issues provided guidance for proposing several possible fuels, including fuel based on low enriched uranium (LEU), reactor-grade plutonium and weapons-grade plutonium.

- The need to accommodate both thermal and fast spectra in significant volumes as well as the need to minimize core size in the case of LEU configurations led us to adopt coupled fast-thermal reactor designs.

In addition to the possibility to generate high fast and thermal neutron fluxes, the use of sodium as coolant in conjunction with a solid moderator opens the door for a highly reconfigurable core. Such a facility could in principle be configured as a fast test reactor only or a thermal test reactor only or as a coupled fast-thermal test reactor depending on the customers' needs. Even though not reported here, this aspect is also being investigated as it provides an additional and important degree of freedom.

The 58 MWt KNK experimental reactor [5] already mentioned above demonstrated that such flexibility is possible. Indeed, it was operated as a sodium-cooled thermal neutron reactor (KNK-I) between 1971 and 1974 when it was shut down and modified to accommodate the new needs of the customers and be able to operate as a fast neutron reactor (with a zirconium hydride moderated driver zone). It was operated as a fast reactor (KNK-II) between 1977 and 1991 when it was permanently shut down. Figure 5.1 below illustrates the KNK-I and KNK-II core configurations. KNK-I fuel elements were cylindrical and made up of a central zirconium hydride moderator section surrounded by 44 fuel rods arranged in two rings, and an outer moderator ring. KNK-II driver fuel elements were hexagonal; the moderated ones contained each 126 fuel rods and 37 zirconium hydride rods and the non-moderated ones contained each 163 fuel rods (both also contained 6 structural rods).

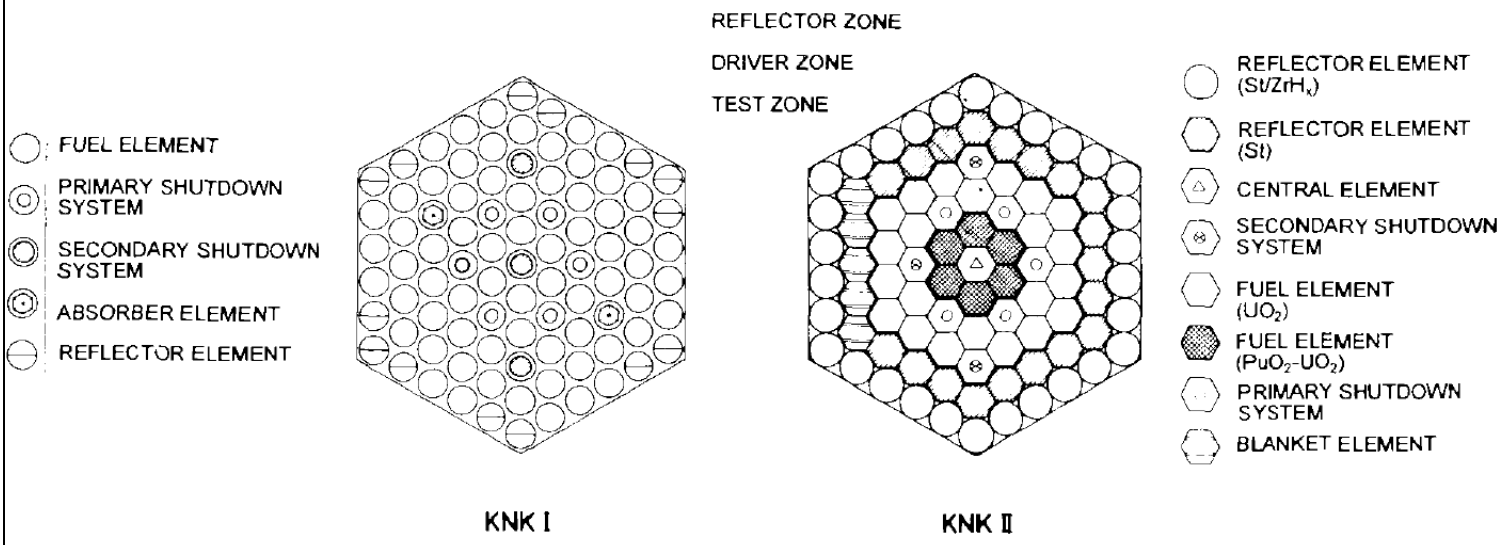

Figure 5.1. Illustration of the KNK-I and KNK-II core configurations [5]

The existing KNK-I plant established narrow limits for KNK-II in respect of its thermal power, coolant flow, and permissible pressure loss. Also the fundamental lattice of the core elements and the positions of

[1] Disposal of irradiated beryllium is complicated by activation products, which include tritium from the beryllium itself, beta-emitting isotopes from common impurities such as nitrogen-14 and niobium-93, and alpha emitting transuranic isotopes from uranium impurity.

the absorbers were to be adopted from KNK-I; only the central secondary shutdown position was cleared for one test element. The result of all these considerations was a two-zone core with 29 fuel elements. The inner test zone with seven fuel elements was to ensure the test conditions, while the outer driver zone had to provide criticality. As the KNK-II core was smaller than the thermal KNK-I core, an additional five blanket elements could be accommodated on external lattice positions.

6. Computer codes used for physics and thermal analyses

Physics analyses.

The current steady-state neutronics calculations were performed using the beta testing version (Serpent2) of the three-dimensional continuous-energy Monte Carlo reactor physics burnup calculation code Serpent [6], which is developed at VTT Technical Research Centre of Finland. Serpent code is also used for the group constant generation for deterministic reactor simulator calculations for safety calculations.

A few changes were necessary to support the Serpent code in calculating the coupling coefficients as described in Avery's formulation. The changes to the code were performed with the help of Dr. Manuele Aufiero from UC Berkeley. A new parameter called "region" is added to the material definition that describes which region this material belongs to. The coupling coefficients are calculated by tracking the neutrons that cause fission.

A deterministic model of a coupled reactor was also prepared and the results of diffusion and transport calculations obtained with the INL-developed MAMMOTH tool compared to those obtained with Serpent. The objective of these analyses was to determine whether or not a deterministic route would be reasonable at a later stage to perform depletion or transient analyses. The preliminary results obtained so far show that it would indeed be a good option. Results are presented in **Appendix C**.

Thermal analyses.

Steady states and transients analyses were performed with RELAP5-3D. RELAP5-3D is the latest in the RELAP5 code series developed at INL for the analysis of transients and accidents in water–cooled nuclear power plants and related systems as well as the analysis of advanced reactor designs. The RELAP5–3D code is an outgrowth of the one-dimensional RELAP5/MOD3 code developed at the INL. The most prominent attribute that distinguishes RELAP5–3D from its predecessors is the fully integrated, multi-dimensional thermal-hydraulic and kinetic modeling capability.

RELAP5-3D was developed for thermal-hydraulic analysis of light water reactors and related experimental systems. The bulk of the validation performed for the code has been for light water systems. Therefore, the applicability and validation of the code for fast reactors cooled by liquid metals will be addressed briefly here. The applicability of important models and correlations in the code for the simulation of reactors cooled by sodium was evaluated in Reference [7]. Validation of RELAP5-3D for subchannel analyses of sodium-cooled fuel assemblies is described in Reference [8]. Validations of RELAP5-3D using EBR-II tests are described in References [9] and [10]. RELAP5-3D has also been used to simulate fast reactors cooled by other liquid metals (lead-bismuth) as described in References [11] and [12].

7. Neutronics analysis of an LEU configuration aiming at minimizing core power and fissile inventory

The core design presented below is far from optimized and will continue to evolve, but, even though more analyses are necessary to quantify it further, it shows that an LEU coupled core design could be made smaller than a more standard LEU fast test reactor design. Indeed, the thermal zone acts as a **booster** (see Section 3, Figure 3.3, for a discussion of boosted configurations) for the fast zone, hence allowing the system to be critical. Cost savings are anticipated by operating a test reactor with a smaller thermal power as well as a smaller mass of fissile material. Simplifications are also anticipated if the test reactor does not have to rely on the use of a (weapons-grade) plutonium-based fuel.

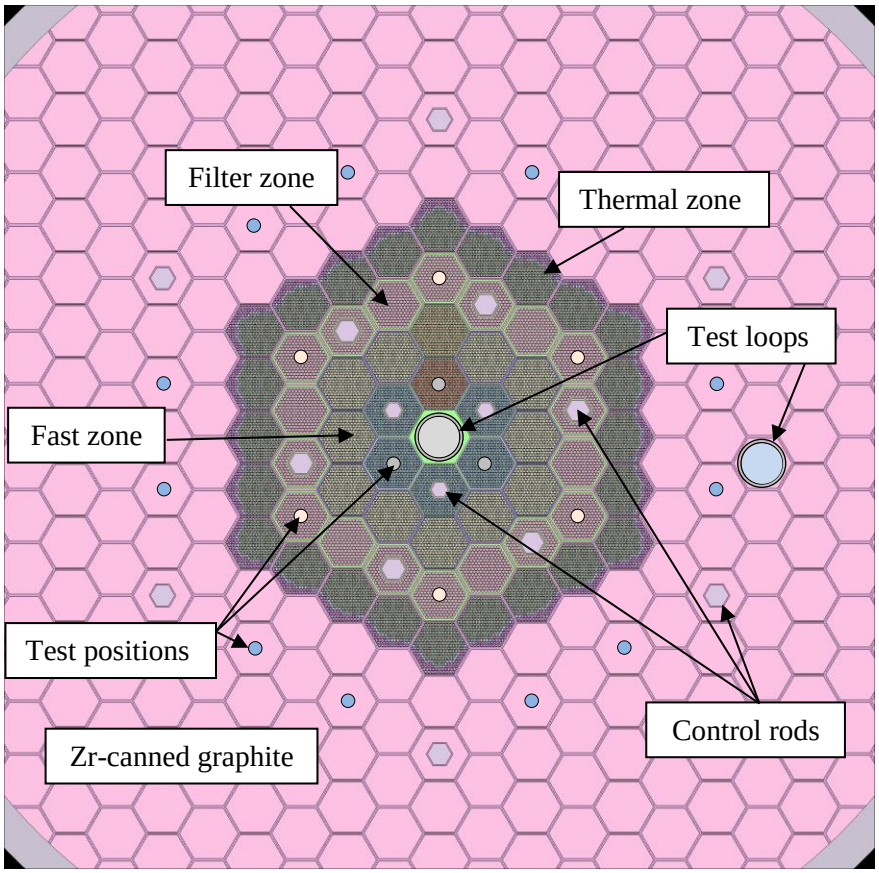

Figure 7.1. Illustration of a 270 MW LEU coupled core configuration

In the 270 MW sodium-cooled core configuration illustrated on Figure 7.1, the fast and thermal zones contain, respectively, 18 and 24 fuel assemblies. A buffer/filter zone made up of steel rods is located between the fast and thermal zones and minimizes the number of thermal neutrons entering the fast zone. The neutron thermalization is provided at the periphery of the active core by graphite blocks canned in zircaloy.

The power in the fast and thermal zones is, respectively, 110 MW and 160 MW. Each fuel assembly has a flat-to-flat dimension of 12.2 cm and contain 271 6.1-mm-diameter U6Zr fuel pins—UZr alloy containing 6 w% Zr and characterized by a density of 16.3 g/cc and a 75 percent smeared density—arranged on a triangular pitch spaced by 0.9 mm diameter wire wraps. The element bundle is contained within a 3-mm-thick hexagonal duct. The fuel, coolant (sodium) and structure volume fractions in the active region of the core are, respectively, 0.47, 0.30 and 0.23. The fuel volume fraction of 0.47 is to be understood as the volume fraction within the clad inner diameter; it includes 0.35 of actual fuel material and 0.12 of gap to accom-

modate fuel expansion. Figures 7.2a and 7.2b provide an illustration of a representative VCTR fuel assembly configuration.

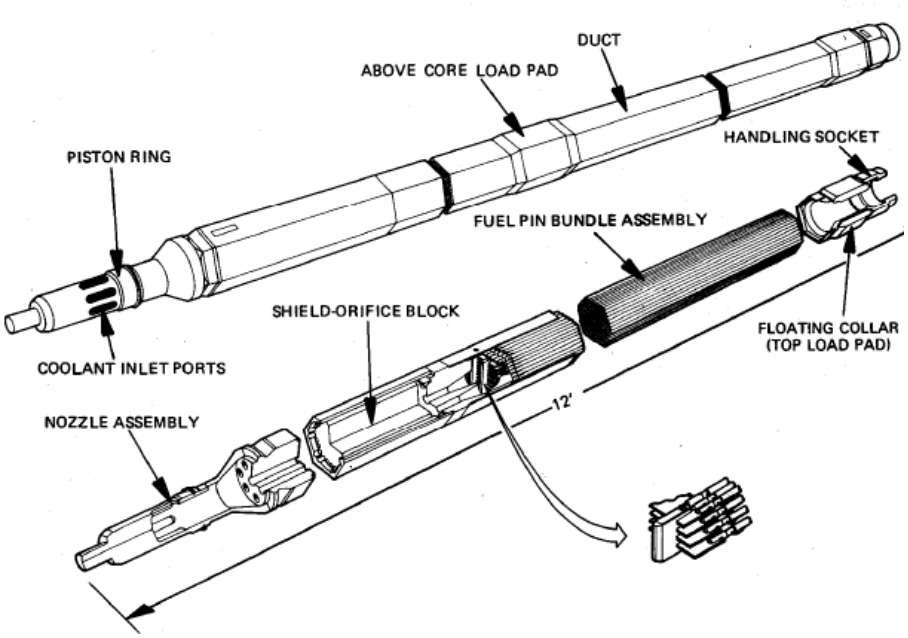

Figure 7.2a. Illustration of a representative VCTR fuel assembly configuration

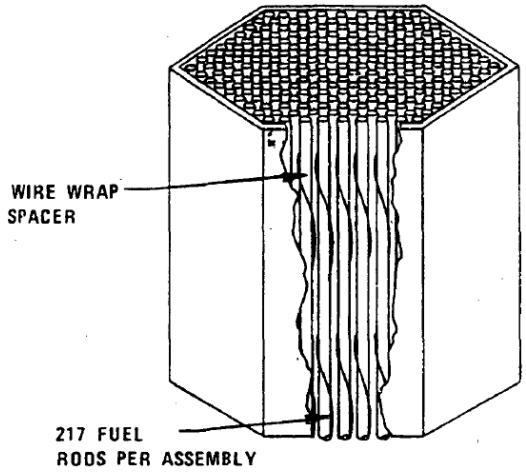

Figure 7.2b. Illustration of a representative fuel pin arrangement in a VCTR fuel assembly

Figure 7.1 shows possible positions for test loops as well as for more standard irradiation positions. Assuming the test loop inner diameter is 11 cm, similar to that of ATR largest flux traps, the useful test volume is about 9.5 liters (1 meter high). The dimensions of the standard irradiation positions have not been defined yet but a diameter of a few centimeters would be typical (also 1 meter high). Note that if the central zone is not occupied by a test loop a fuel assembly could be present.

The LEU inventory in the core is approximately 2.85 tonnes. The use of a high density fuel is necessary to ensure the system is critical; metal fuel has been considered the reference so far but preliminary calculations show that uranium nitride fuel would also work if it was enriched in nitrogen-15 to a level of at least 90 percent. In order to be critical and meet the flux level requirement, a core using a lower density fuel,

such as uranium dioxide, would be larger and, consequently, its power would also be larger; this option has not been considered further in this study.

As mentioned above, sodium is used to cool the reactor. The inlet and outlet temperatures currently considered are, respectively, 350°C and 500°C, i.e. prototypic of most sodium-cooled fast reactor designs. These temperatures could, and will, probably be modified as optimization of the design progresses. For example, if necessary, lowering the inlet temperature and increasing the ΔT across the core would reduce the sodium velocity[1] and associated pressure drop.

In the fast zone, assembly ducts and fuel clad are made up of steel, whereas in the thermal zone, assembly ducts are made up of zircaloy to minimize neutron absorption and fuel clad is made up of steel. The active fuel height in both fast and thermal zones is 1 meter; the gas plenum in both zones is 30 cm high. The average power density in the active part of the core is 515 kW per liter and the average linear power is 24 kW per meter. Using one single fuel enrichment (19.9 percent), the power distribution is relatively flat in the fast zone; the peak linear power is 31 kW per meter. On the other hand, a zoning of the fuel enrichment is necessary at the periphery of the core, at the interface with the graphite reflector, to ensure the fuel integrity; three fuel enrichments (3, 7 and 19.9 percent; 15.0 percent average, see Figure 7.3) are used and the hottest fuel rod linear power is 41 kW per meter. Optimization is under way and the fuel assembly characteristics will probably continue to evolve.

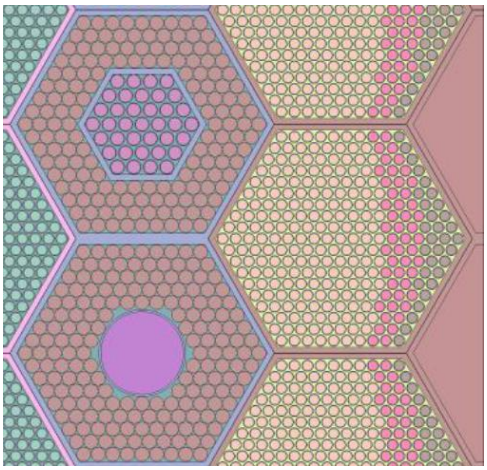

Figure 7.3. Close up showing the 3 enrichment zones in the fuel assemblies next to the graphite reflector

The peak fast flux (above 0.1 MeV) at the center of the fast zone, where a test loop could be located, is 3.5×10^{15} n/s.cm^2 which corresponds to about 31 displacements per atom[2] (dpa) per year (assuming 300 days of operation at full power per year). For reference, the fast flux obtained in the 140 MW test reactor JOYO [**13**] is about 4×10^{15} n/s.cm^2 but in a smaller volume. Work is underway to increase the VCTR peak fast flux further. The fast flux in the three test locations near the central position is also about 3.5×10^{15} n/s.cm^2. The unperturbed peak thermal flux (below 0.625 eV) in the graphite reflector is about 10^{15} n/s.cm^2, about twice what is currently achievable in ATR flux traps. Such a high thermal neutron flux associated with large irradiation volumes, would allow efficient isotopes production. Figure 7.4 shows the neutron spectra that are available in the current design.

[1] Coolant velocity must be less than the limits dictated by flow-induced vibration, cavitation, and corrosion-erosion considerations. For FFTF and CRBR these were conservatively established at 30 ft/s (9m/s) for non-replaceable components, 40 ft/s (12 m/s) for replaceable components in the high temperature low pressure region and 50 ft/s (15 m/s) for replaceable components in the low temperature, high pressure, or inlet region.

[2] In radiation material science the displacements per atom in a solid is considered a better representation of the effect of irradiation on materials properties than the neutron fluence.

Table 7.1. Fuel, reflector, control and moderator assembly physical parameters

	Thermal	Fast	Control (buffer/ Thermal)	Control (Fast)	Reflector	Thermal Moderator
Assembly Data						
Number of pins	271	271	37	19	SS (217)	Graphite
Assembly pitch, cm	12.245	12.245	N/A	N/A	12.245	12.245
Duct materials	Zr	HT9	HT9/Zr	HT9	HT9	Zr
Duct thickness, mm	3	3	3	3	3	3
Pin Data						
Slug alloy	U10%Zr	U6%Zr	B_4C	B_4C	N/A	NA
Pin Length, mm	100	100	100	100	N/A	NA
Slug smeared density, %TD	75	75	85	85	N/A	NA
Slug diameter, mm	5.4	5.4	6.4	6.4	N/A	NA
Cladding alloy	HT9	HT9	HT9	HT9	HT9	NA
Clad outer diameter, mm	6.1	6.1	6.8	6.8	6.8	NA
Pin pitch-to-diameter, ratio	1.15	1.15	1.09	1.09	1.09	NA
Cladding thickness, mm	0.35	0.35	0.2	0.2	N/A	NA
Wire wrap diameter, mm	0.91	0.91	0.6	0.6	0.6	NA

The optimization of the cycle length is currently underway; preliminary estimates show that a cycle length of about 75 days is possible with a third of the core being unloaded at each cycle. Peak pin burnup are of the order of 4 percent. Because the uranium-235 enrichment is limited to 20 percent, limiting parasitic neutron absorption is essential to increase the cycle length. For example, replacing steel by zircaloy in the buffer zone increases the reactivity of the system by about one percent Δk and replacing steel by zircaloy for the fuel clad in the thermal zone increases the reactivity by about another one percent Δk. Given the burnup reactivity swing of the system of about 21×10^{-5} Δk per day, a one percent Δk increase translates into approximately a 71-day increase of the fuel residence time, or, equivalently, a 23.5-day increase of the cycle length. The use of burnable poison in the thermal region—not considered here—should reduce the burnup reactivity swing of the system and ease the control requirement.

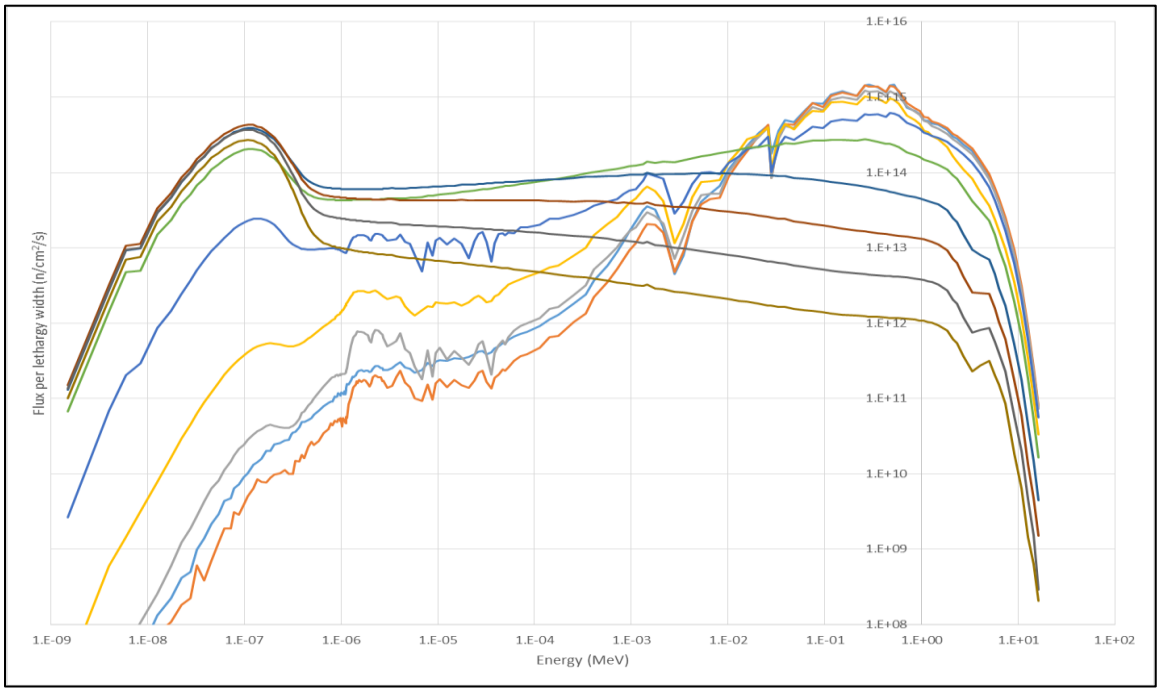

Figure 7.4. Neutron spectra available in VCTR.

Note that modifications to the JOYO core have also been investigated [14] to increase the core burnup and to improve the irradiation efficiency. Among the various options considered, the replacement of the radial reflector elements made of stainless steel with elements made of zirconium alloy or nickel-based alloy showed effective in increasing the reactivity and, consequently, the cycle length. The replacement was found to provide a reactivity increase of about 0.41 and 0.44 percent Δk, respectively.

In the VCTR configuration shown on Figure 7.1, the fast and thermal zones are very tightly coupled as demonstrated by the calculated neutronic parameters: k_F = 0.73, k_T = 0.75, k_{FT} = 0.36 and k_{TF} = 0.18. The k_{eff} of system loaded only with fresh fuel is 1.045. Each zone is very subcritical on its own whereas the coupling ensures the system is critical. Every fission neutron born in the fast zone generates on average about 0.36 fission neutron in the thermal zone whereas every fission neutron born in the thermal zone generates on average about 0.18 fission neutron in the thermal zone. From these results it is concluded that the core configuration presented in Figure 7.1 has a SVP parameter of about 2, which demonstrates a strong coupling and limited flux tiltiness (see Appendix B).

Movable absorbers are necessary to control the burnup reactivity swing and ensure at least a 5 percent Δk_{eff} margin at cold shutdown. The total movable absorber reactivity worth is core specific but a value of 10 percent Δk_{eff} is typical to guarantee the above criteria are met. The calculations performed considering the preliminary control rod pattern shown in Figure 7.1 above demonstrate that this can be achieved using a combination of control rods in the fast zone, in the buffer zone and at the periphery in the graphite. The material used for the control rods is the standard boron carbide (B_4C) 80 percent enriched in B-10.

Table 7.2. Control rod reactivity worth

	$\Delta k_{eff} \times 10^2$
CR in graphite (6)	-4.8
CR in fast zone (3)	-3.0
CR in filter (6)	-7.4
CR in fast zone and graphite (9)	-5.9
CR all in (15)	-12.7

Several reactivity coefficients are presented in Table 7.3 below. First and foremost, the sodium void reactivity coefficients calculated are either negative or only slightly positive; the total loss of sodium results in a 2.0 percent Δk decrease of the reactivity, whereas the loss of sodium in the fast zone only results in a 2.1 percent Δk decrease of the reactivity. On the other hand, the loss of sodium in the thermal zone only results in slight increase of the reactivity (less than 0.2 percent Δk).

Table 7.3. Reactivity coefficients of the LEU coupled core

	$\Delta k_{eff} \times 10^2$
All Void	-2.01
Fast Void	-2.13
Thermal Void	0.17
5% Axial Exp (Δh = 5 cm)	-0.60
10% Axial Exp (Δh = 10 cm)	-1.31
Radial Exp (ΔPitch = 0.1 cm)	-0.81
Doppler (ΔT = +300K)	-0.19
Fast only Doppler (ΔT = +300K)	-0.05
Thermal only Doppler (ΔT = +300K)	-0.15

The effect of a uniform core radial expansion[1] on the reactivity was calculated by increasing the assembly pitch by 0.1 cm, i.e. by increasing the distance between the fuel assemblies while keeping the assembly dimensions unchanged. This increases the core radius and volume by, respectively, 0.8 percent and 1.6 percent. The effect on the reactivity is negative (–0.81 percent Δk, see Table 7.3) and corresponds to approximately –1 percent Δk for a 1 percent increase of the core radius.

The effect of a uniform core axial expansion on the reactivity was also calculated by increasing the fuel axial dimension by 5 cm and 10 cm. The reference fuel height being 100 cm, it corresponds to an increase of core height (and volume) of 5 and 10 percent. The effects are negative and approximately linear: –0.6 percent Δk for 5 cm and –1.3 percent Δk for 10 cm (see Table 7.3). It corresponds to –0.12 percent Δk for a 1 percent increase of the core height. Finally, as expected, the fuel temperature coefficients are negative (between about $-0.17\times10^{-5}\Delta k$/K and $-0.63\times10^{-5}\Delta k$/K).

The effective delayed neutron fraction (beta effective) and prompt neutron lifetime of the system are, respectively, 0.71 percent and 107 microseconds. The prompt neutron lifetime of the coupled core concept is about 200 times larger than that of a more standard fast core. In case of an unprotected prompt reactivity excursion starting at low operating power (e.g. accident due to rapid withdrawal of control rods), the peak power is inversely proportional to the prompt-neutron lifetime. Consequently, the peak pressures and accelerations, caused by material expansion, would be much smaller in the VCTR than in a more standard fast test reactor because of the much longer prompt neutron lifetime. This particular aspect will need to be quantified further as part of the safety evaluation.

As mentioned from the beginning, the current VCTR design is only in a very preliminary stage and is still subject to modifications, some of which could possibly adversely lower the core reactivity. If this is the case, the cycle length will be negatively impacted because the uranium-235 fuel enrichment cannot be increased any further to regain reactivity without crossing the LEU/HEU enrichment limit of 20 percent.[2] If the resulting cycle length is deemed too short, plutonium could also be used in conjunction with LEU in the fast zone as a way to increase the cycle length and fuel burnup, an approach also used in JOYO.[3]

Preliminary calculations show that the addition of one percent of Pu-A or of Pu-B—two plutonium isotopic compositions representative of the material present at INL, see Table 7.4—to the LEU fuel in the fast zone brings about a, respectively, 1.25 and 1.5 percent Δk increase which translates into approximately a 90-day and 105-day increase of the fuel residence time, or, equivalently, a 30-day and 35-day increase of the cycle length. The addition of 1 percent of plutonium to the fuel would require no more than approximately 13 kg of plutonium per year. At this rate—even if a few percent of plutonium were used for the fuel fabrication—there is enough plutonium present at INL to provide an additional source of fissile material for several decades of operation without having to rely on an external source of weapons-grade plutonium.

Table 7.4. Plutonium isotopic composition representative of the material present at INL

	Pu-238	Pu-239	Pu-240	Pu-241	Pu-242
Pu-A	0.1	68.7	26.4	3.4	1.4
Pu-B	0.05	87.2	11.6	1.0	0.15

[1] The uniform radial expansion depends on the change in the dimensions of the lower core support structure as a function of the sodium inlet temperature.

[2] An obvious way to increase the amount of fissile material is to increase the fuel smeared density above the 75 percent considered here. This is however not recommended—and has not been considered here—from a fuel performance point of view.

[3] The 140 MW JOYO fast test reactor requires UO_2-PuO_2 fuel (MOX) containing between 23 and 30 percent of Pu in addition to 18 percent enriched U to ensure a 60-day cycle length [**14**]

8. Neutronics analysis of Pu-LEU configurations

8.1 Configuration aiming at minimizing the plutonium inventory of the fast zone

Using the same geometric configuration as in section 7, analyses have also been performed assuming weapons-grade plutonium (Table 8.1) is used in the fast zone while LEU is used in the thermal zone. The use of plutonium in the fast zone provides more flexibility in the choice of the fuel assembly design than when LEU is used because, the reactivity worth of plutonium being higher than that of uranium-235, the neutron balance is not as tight. For example, if necessary, the fuel volume fraction could be lowered and the sodium volume fraction could be increased in order to facilitate cooling of the fuel, and, possibly, increase the power density and fast neutron flux. This has not been analyzed yet and the fuel assemblies and fuel pins considered in this section have the same dimensions has in section 7. The fuel is UPu6Zr (UPuZr alloy containing 6 w% Zr and characterized by a 75 percent smeared density) in the fast zone and U6Zr in the thermal zone. The plutonium content necessary to reach similar performance as the LEU core described in Section 7 is 14.5 percent; with this configuration the LEU and plutonium inventories are, respectively, about 1.63 tonnes (including 244 kg of uranium-235) and 1.22 tonnes (including 177 kg of plutonium).

Table 8.1. Plutonium isotopic composition considered representative of weapons-grade material

	Pu-238	Pu-239	Pu-240	Pu-241	Pu-242
Pu-WG	-	94	6	-	-

In this 270 MW configuration, the fast and thermal zones are also very tightly coupled as demonstrated by the calculated neutronic parameters: k_F = 0.73, k_T = 0.76, k_{FT} = 0.41 and k_{TF} = 0.16. The k_{eff} of system is 1.045. The same reactivity coefficients as for the LEU-only configuration were also calculated for the plutonium-LEU configuration and are presented in Table 8.2 below. Qualitatively, the trends are similar for the two configurations. As expected, the sodium void reactivity coefficient of the fast zone is less negative when it is loaded with plutonium than when it is loaded with LEU.

The effective delayed neutron fraction (beta effective) and prompt neutron lifetime of the system are, respectively, 0.54 percent and 98 microseconds. As expected, the use of plutonium in the fast zone lowers the effective delayed neutron fraction of the system compared to the case when LEU is used. On the other hand, the use of plutonium has only a very limited impact on the prompt neutron lifetime of the system which remains two orders of magnitude larger than that of a fast neutron system.

Assuming a cycle length of 100 days with one third of the core being replaced at each cycle, this core would require approximately 200 kg of plutonium per year assuming the fuel is not recycled and about one tenth of that if it were.

Table 8.2. Reactivity coefficients of the coupled core with plutonium in the fast zone and LEU in the thermal zone

	$\Delta k_{eff} \times 10^2$
All Void	-0.89
Fast Void	-1.12
Thermal Void	0.30
5% Axial Exp (Δh = 5 cm)	-0.98
10% Axial Exp (Δh = 10 cm)	-1.54
Radial Exp (ΔPitch = 0.1 cm)	-0.86
Doppler (ΔT = +300K)	-0.21
Fast only Doppler (ΔT = +300K)	-0.06
Thermal only Doppler (ΔT = +300K)	-0.15

8.2 Configurations aiming at providing additional control of the irradiation conditions in the thermal zone

In the 300 MW configuration illustrated on Figure 8.1, the fast and thermal zones contain, respectively, 84 and 72 fuel assemblies. The power in the fast and thermal zones is, respectively, 165 MW and 135 MW. Each fuel assembly in the fast zone has a flat-to-flat dimension of 7.0 cm (i.e. smaller than in the configuration presented above) and contains 91 6.0-mm-diameter UPu20Zr fuel pins arranged on a triangular pitch spaced by wire wraps. The element bundle is contained within a 1-mm-thick hexagonal duct. The fuel, coolant (sodium) and structure volume fractions in the active region of the core are, respectively, 0.41, 0.36 and 0.23. The fuel volume fraction of 0.41 is to be understood as the volume fraction within the clad inner diameter; it includes 0.307 of actual fuel material and 0.103 of gap to accommodate fuel expansion.

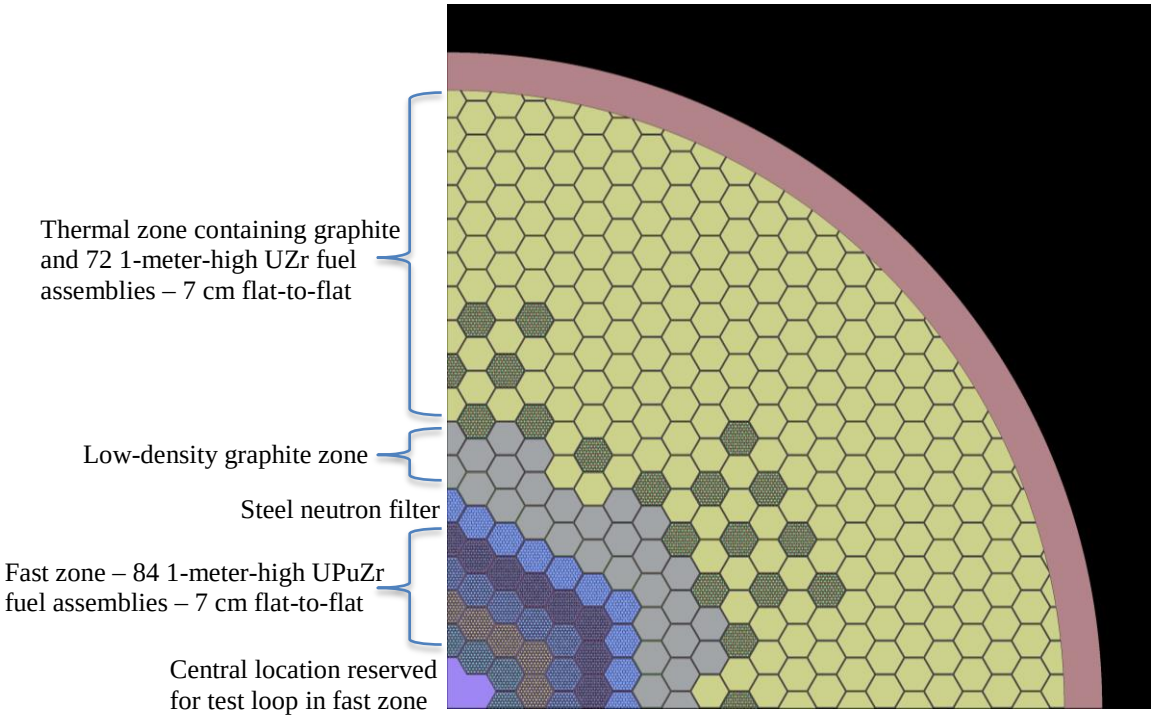

Figure 8.1. Illustration of a 300 MW Pu-LEU coupled core configuration

This central zone is surrounded by a graphite-moderated and sodium-cooled thermal zone with U10Zr metal fuel in similar fuel assembly as in the fast zone except that they contain 6 burnable poison pins located at the corners of the assembly and 19 graphite pins to increase the moderation within the assembly, i.e. each thermal zone assembly contains 66 fuel pins (Figure 8.2). The burnable poison is used both to reduce the reactivity swing during the depletion cycle and also to reduce the effect of the sodium voiding. The fixed absorbers present in the thermal region reduces the contribution of sodium to the overall neutron absorption in the core, thus reduces the effect when the absorber (sodium) is lost from the system.

A steel neutron filter is placed between the two regions to keep thermal neutrons from entering the fast zone. A low-density graphite region separates the thermal and the fast zones, which enables the fast neutrons to reach to either zone without being slowed down to thermal energies to improve the coupling between the regions. The graphite in the intermediate region is canned with zirconium containing 5% hafnium as impurity to enhance the filtration of the thermal. A test location (closed loop) is at the center of the fast zone, which is surrounded by 4 rings of fast fuel assemblies (84 assemblies). A total of 72 thermal fuel assemblies are located in the graphite moderator blocks as clusters of 11 as shown in Figure 8.1. The large volume between the clusters of the thermal fuel assemblies are reserved for the 6 large thermal zone test

locations. A potential advantage of such a configuration is that it may allow a better control of the irradiation conditions in the thermal zone and minimize flux gradients.

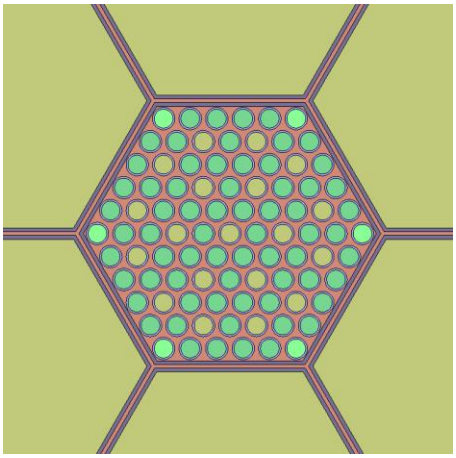

Figure 8.2. Illustration of a thermal fuel assembly with 6-burnable poisons and 19-moderator pins.

The plutonium content in the fast zone is 20 percent while the uranium-235 enrichment in the thermal zone is 11.5 percent. No enrichment zoning calculations for the thermal zone have been performed so far. Both fast and thermal fuel pins have standard stainless steel clad, however, in order to minimize parasitic neutron absorption, the thermal fuel assembly cans are made up of zirconium whereas the fast fuel assembly are made up of stainless steel.

With this configuration, the LEU and UPu inventories are, respectively, about 1.0 tonnes (including 115 kg of uranium-235) and 1.5 tonnes (including 300 kg of plutonium); preliminary estimates show that a cycle length of about 80 days is possible with a third of the core being unloaded at each cycle. Because the core is more "spread out" than the other geometric configuration, the fast and thermal zones are not as tightly coupled as demonstrated by the calculated neutronic parameters: k_F = 0.92, k_T = 0.63, k_{FT} = 0.10 and k_{TF} = 0.26. The k_{eff} of system is 1.018. Whether or not this level of coupling is sufficient to ensure the stability of the flux distribution will need to be demonstrated.

The current design has one loop position in the center of fast zone. The number and exact locations of the test loops in the thermal zone is still a work in progress, however there are 6 possible locations between the fuel assembly clusters. There will also be numerous more standard positions for fuels and material tests that do not require loops. The fast flux (above 0.1 MeV) in the fast zone irradiation location is about 4.0×10^{15} n/cm^2.s, while the thermal flux (below 0.625 eV) in one of the possible irradiation locations reaches about 7.8×10^{14} n/cm^2.s. Analyses are underway to increase the fast neutron flux level further. Using better moderator pins in the graphite reflector around the test locations such as ZrH pins can further increase the thermal flux.

Figure 8.3 illustrates another configuration with 2 loops in the fast zone. The power, flux levels and cycle length obtained with this configuration are similar to those presented above. Figure 8.4 shows the flux map calculated by Serpent.

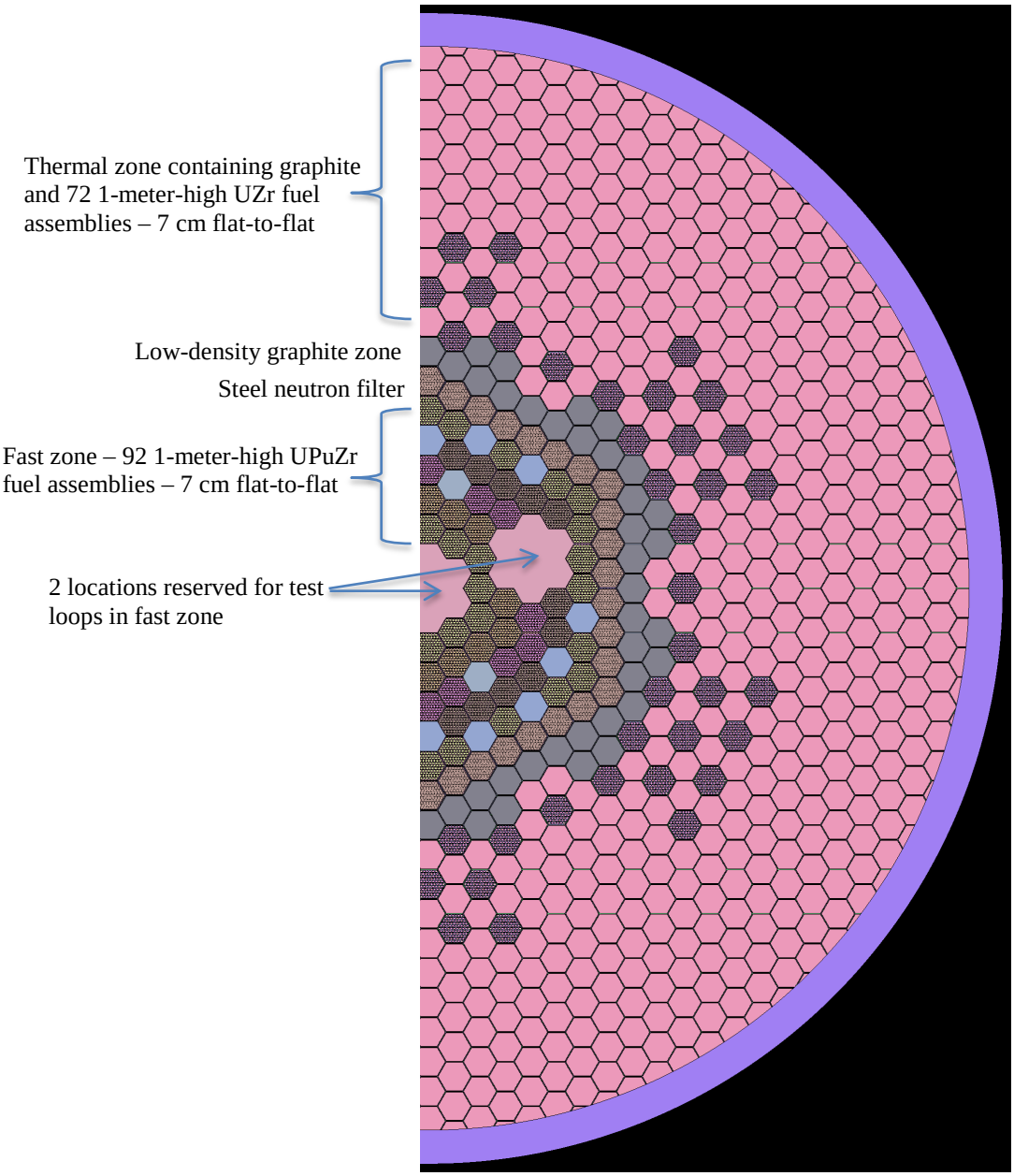

Figure 8.3. Illustration of a 300 MW Pu-LEU coupled core configuration with 2 loops in the fast zone

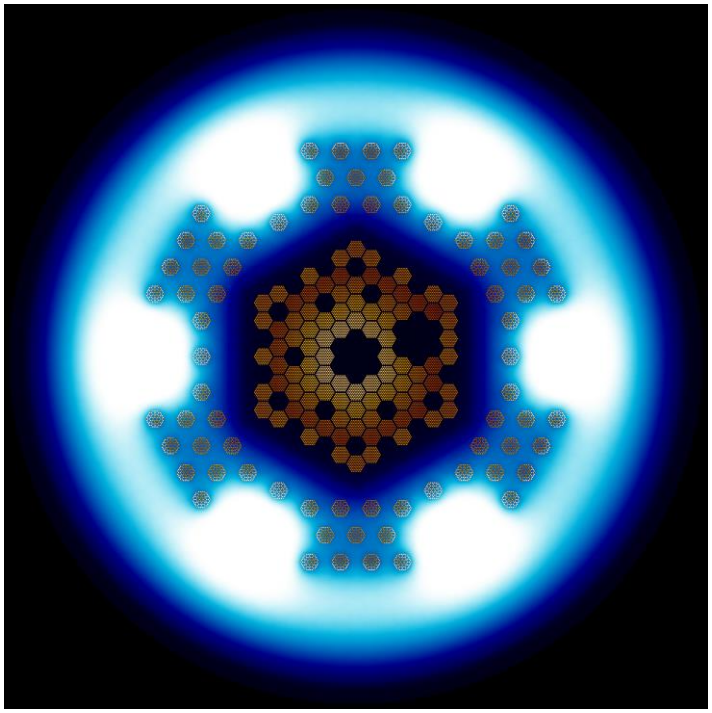

Figure 8.4. Flux map calculated by Serpent for the 2-loop configuration

9. Preliminary thermal analyses

A RELAP5-3D model of the VCTR was developed. The model represents the primary coolant system and a portion of the secondary coolant system. The primary coolant system consists of the reactor, the reactor tank, and two external coolant loops. The model uses six one-dimensional channels to represent the active core, including average-powered, low-powered, and high-powered assemblies in the fast and thermal cores. The power in the low-powered assemblies is reduced by 10% compared to the average whereas the power in the high-powered assemblies is increased by 10%. The geometry of the flow channels through the core is based on a flat to flat dimension of 12.225 cm. Flow channels are also used to simulate the side reflector and the graphite assemblies. An orifice was used in the side reflector to reduce the flow to about 6% of the total. The flow through the graphite assemblies is less than 1% of the total. The model of the reactor tank is based on geometry described in Section 11.

The model also represents two external primary loops. Each external loop contains an intermediate heat exchanger (IHX), a centrifugal pump, and piping. These loop components were scaled from the JOYO reactor described in Reference [15]. Full height power-to-volume scaling was used to obtain dimensions in the loops. With this scaling approach, flow areas are proportional to the core power. Reference [15] did not contain much information on lengths and elevation changes of most components. Therefore, these values were generally guessed at. The hot leg, pump suction, and cold leg lengths were assumed to be about 20 m long. The elevation change within the loop was varied parametrically as described later.

The model applies flow and inlet temperature boundary conditions on the secondary side of each IHX. Input data for the secondary side of the IHX are also scaled from JOYO. The overall performance of the model at steady-state is summarized in Table 9.1. The inlet temperature on the secondary side of the IHX was adjusted to obtain a cold leg temperature of 350°C. The primary-side flow rate was adjusted to obtain a hot leg temperature of about 500°C. Table 9.2 summarizes the performance of the reactor at steady state. Orifices were placed in the flow channels in the fast core so that the fluid temperatures at the exit of the fast and thermal channels were about the same.

Table 9.1. System parameters at 100% power.

Parameter	Value
Primary side:	
Core power, MW	266.6
Total primary mass flow rate, kg/s	1388
Cold leg temperature, °C	350
Hot leg temperature, °C	501
Secondary side:	
Total secondary mass flow rate, kg/s	1270
IHX inlet temperature, °C	293
IHX outlet temperature, °C	457

The calculated peak cladding temperature is 533°C. Fast reactors typically have a large temperature variation within an assembly due to subchannel and hot pin effects. The temperature in the worst subchannel is typically about 50°C higher than the average temperature. After accounting for subchannel effects, the estimated peak cladding temperature for the current design is about 533 + 50 = 583°C, which should be acceptable since the steady-state temperature limit is likely to be 600°C or slightly higher.

Historically, the maximum pressure drop across the assemblies has been limited to about 80 psi (0.55 MPa). The calculated pressure drop across the assemblies is 0.88 MPa, which is considerably higher than

historically allowed.[1] Removing the orifices in the fast assemblies reduced the differential pressure across the assemblies to 0.79 MPa, but increased the maximum cladding temperature by 11°C. Increasing the flow area in the assemblies by about 20% would reduce the differential pressure to the historical value, but would probably degrade the nuclear performance of the reactor. The design should be optimized in a manner that considers both the nuclear and thermal-hydraulic performance of the reactor.

Table 9.2. Reactor parameters at 100% power.

Parameter	Fast Core	Thermal Core	Side Reflector	Graphite
Assemblies	18	24	18	267
Power, MW	104.0	162.6	0	0
Lengths, m				
Grid	0.36	0.36		
Shielding	0.60	0.60		
Active fuel	1.00	1.00		
Gas plenum	0.28	0.28		
Handling tool	0.30	0.30		
Total	2.54	2.54	2.54	2.54
Primary loop parameters:				
Tin, °C	350	350	350	350
Tout, °C	511	511	350	350
Peak clad temperature, °C	532	533		
Peak fuel temperature, °C	613	640		
Flow, kg/s-assembly	28.2	33.1	4.43	0.02
Maximum assembly velocity, m/s	9.30	10.9	1.33	0.43
Core differential pressure, MPa	0.88	0.88	0.88	0.88

An orifice was modeled at the inlet to the side reflector to limit the flow through it. Without the orifice, more than 30% of the total flow went through the side reflector. The pitch-to-diameter ratio of the stainless steel pins in the current model is 1.088. Reducing the pitch-to-diameter ratio would result in the use of a larger orifice, but would otherwise not affect the thermal-hydraulic response of the reactor. Reducing the pitch-to-diameter ratio would likely improve the nuclear performance of the reactor. Thus, the optimization of the design should also consider the pitch-to-diameter ratio of the stainless steel pins in the side reflector.

A protected loss of flow transient was simulated with the model. The elevation change (dZ) between the centers of the core and IHXs was varied parametrically to determine the effect of the elevation change on the transition to natural circulation. The elevation changes varied from 9.1 m to 5.3 m. The former value placed the IHX about 2.8 m above the top of the reactor tank, while the latter value placed the IHX about 1.0 m below the top of the tank. Smaller elevation changes were judged not to be credible. The loop piping could be designed to provide larger elevation changes if necessary. Figure 9.1 shows maximum cladding temperature as a function of time. With an elevation change of 9.1 m, the maximum cladding temperature increased above the steady steady-state value but remained below the anticipated steady-state temperature limit of 600°C. The peak cladding temperature was 633°C when the elevation change was reduced to 4.3 m.

Figure 9.2 compares the calculated flow at the inlet to the core with the flow from a theoretical flow coastdown with a halving time of 6 s. Natural circulation flow is fully established by 40 s with the elevation change of 9.1 m. The elevation change between the core and the IHX significantly affects the magnitude of the natural circulation flow and somewhat affects the variation in flow between channels as shown in Fig-

[1] Note, however, that the IAEA reference [15] mentions that both BN-350 and BN-600 operate (or operated) with a pressure drop of 0.7 MPa

ure 9.3. The natural circulation flow rate was about 30% larger with the larger elevation change. A 10% variation in power per channel caused the flow rates per channel to vary by about 1% with the larger elevation change and by about 2% with the smaller elevation change.

Figure 9.4 compares the calculated power from a point kinetics model with the power removed by the IHXs. The flow on the secondary side of the IHXs was reduced to 1.9% of the initial value, within 10 s. The 1.9% value corresponds to the decay heat removal capabilities given for JOYO [14]. The core and IHX powers were nearly equal by 100 s.

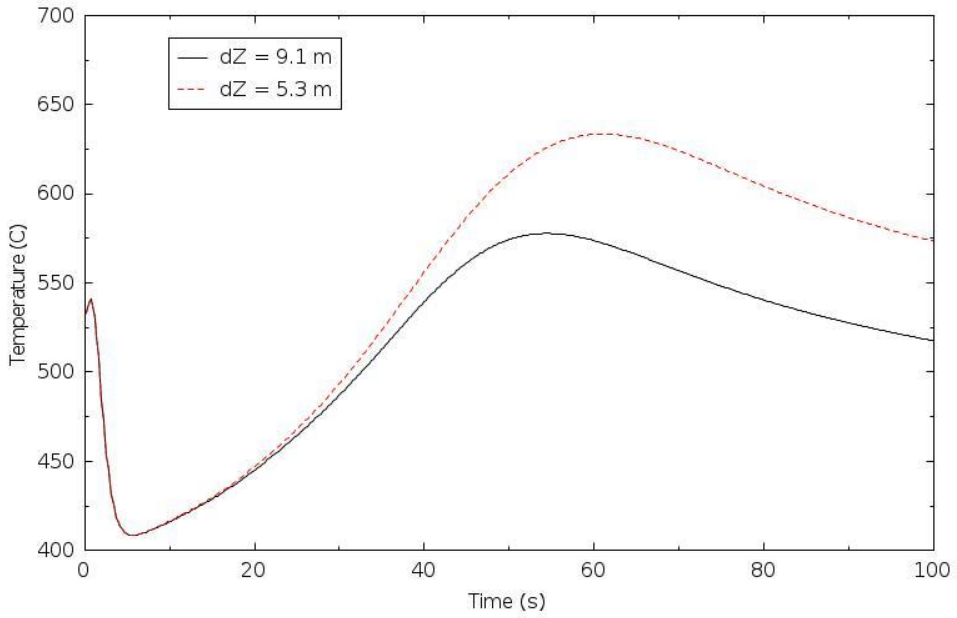

Figure 9.1. Maximum cladding temperature as a function of time and elevation change during a protected loss of flow transient.

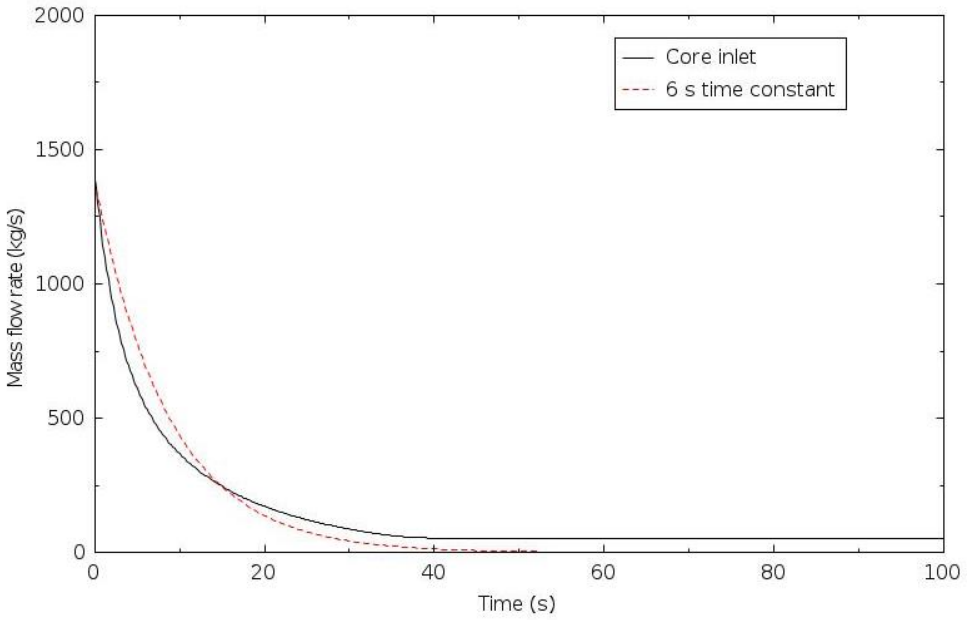

Figure 9.2. Calculated flow rates during the protected loss of flow transient (dZ = 9.3 m).

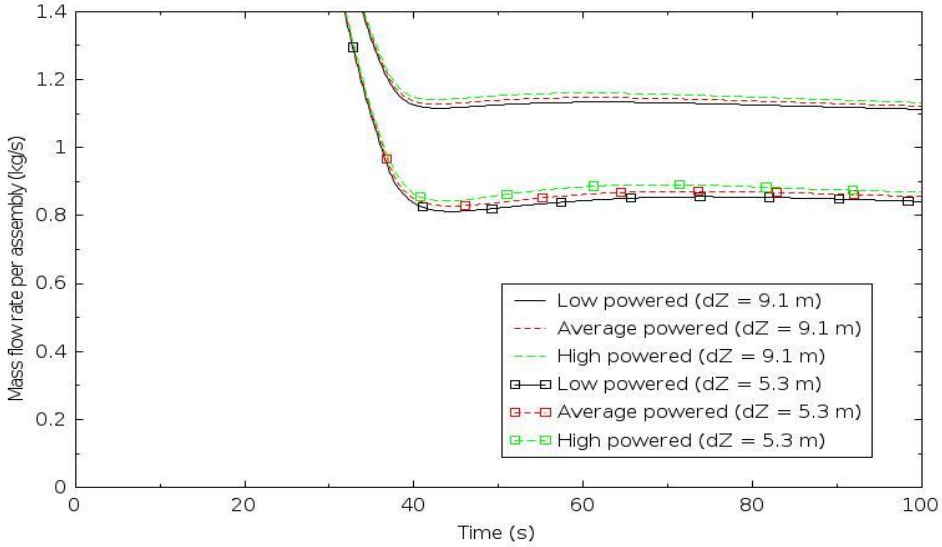

Figure 9.3. The effect of elevation change on channel inlet flows.

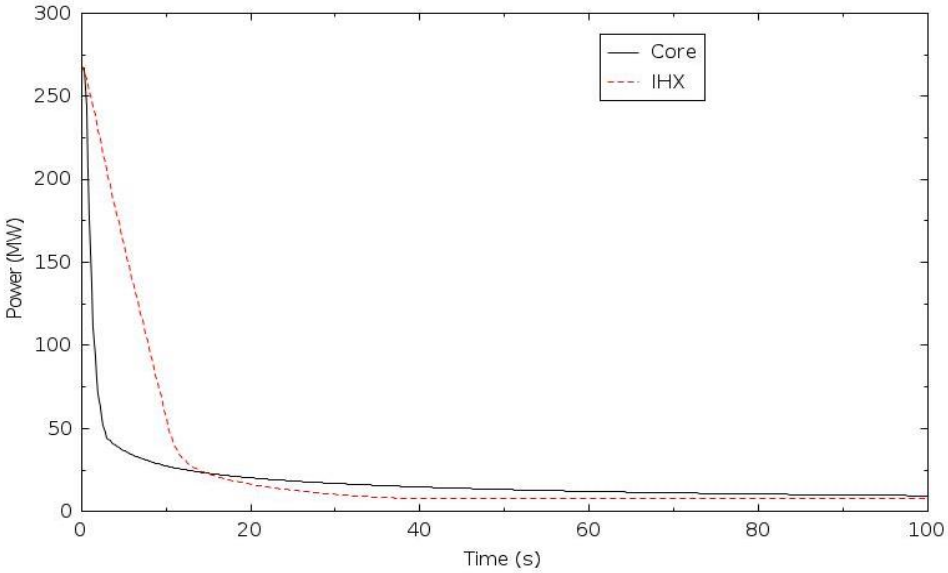

Figure 9.4. Calculated core and IHX power during a protected loss of flow transient.

A protected loss of heat sink transient was simulated with the RELAP5-3D model. The transient was initiated by linearly decreasing the flow on the secondary side of the IHXs to zero in 10 s. Two calculations were performed, one in which the primary coolant pumps continued to operate and one in which they coasted down. The latter calculation corresponds to a station blackout. No decay heat removal systems were assumed to operate. This calculation provides an indication of the time required for the decay heat removal system to operate during a blackout. Maximum cladding temperatures are shown in Figure 9.5.

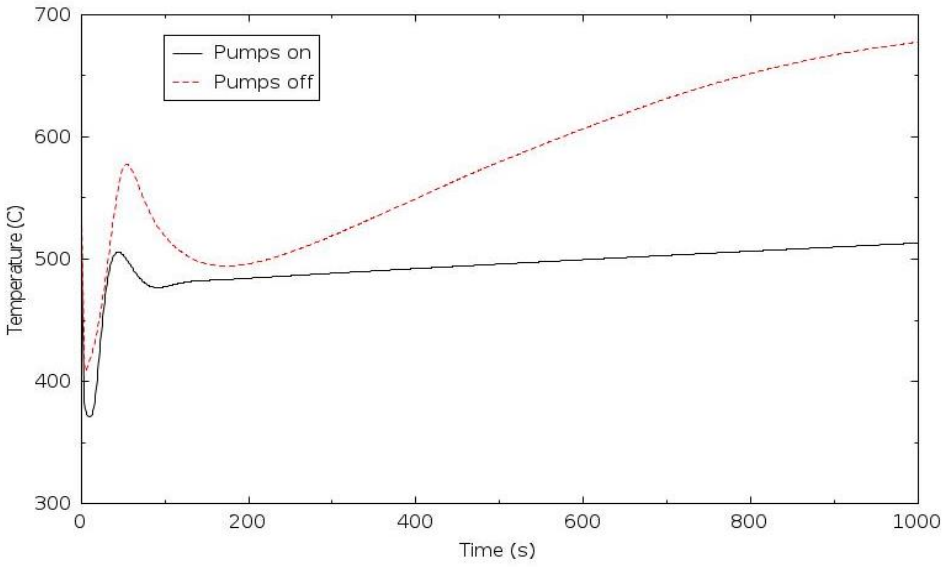

Figure 9.5. Maximum cladding temperature during a protected loss of heat sink transient.

With the primary coolant pumps running, the peak clad temperature decreased rapidly following scram and then increased as the hot fluid initially in the upper plenum and hot legs flowed around the primary circuit and reached the core. The temperature increased monotonically after 200 s due to decay heat and pump power. With the primary coolant pumps tripped, the initial response was similar to that shown previously for the loss of flow. The maximum cladding temperatures then increased due to the lack of decay heat removal. Assuming that the maximum cladding temperature should be kept below 600°C, the calculations show that the decay heat removal systems are not required to operate until about an hour following the loss of heat sink, but are required within 10 minutes in the blackout.

Steady-state calculations were also performed to determine the effect of variations in core power on average fuel temperatures. These calculations were performed to provide input to the reactor kinetics feedback calculations. The results at 100% power (266.6 MW) were taken from the same calculation described in Tables 9.1 and 9.2. The second calculation was done at 101% power. The third calculation was performed at 110% power to check for linearity. The core inlet temperature and mass flow rate were held constant in all three calculations so that the results depended only on changes within the core and not the systems used to control the behavior of the IHX and primary coolant pumps. The results of the calculations are shown in Table 9.3. A 1% increase in core power caused the average fuel temperature to increase by 1.48°C in the fast core and by 1.61°C in the thermal core. A 10% increase in core power caused the average fuel temperature to increase by 14.75°C in the fast core and 15.97 °C in the thermal core. Thus, the change in temperature was nearly linear with respect to power. The change in temperature in the thermal core was higher than in the fast core because the linear heat generation rate was higher in the thermal core and a given percentage change in power resulted in a larger absolute change in linear heat generation rate. The lower thermal conductivity of the fuel in the thermal core (U-10Zr) compared to the fast core (U-6Zr) also contributed to the larger rate of temperature increase in the thermal core.

Table 9.3. Average fuel temperatures at steady state.

Total power (MW)	Average fuel temperature (°C)	
	Fast core	Thermal core
266.6	503.75	518.77
269.266	505.23	520.38
293.26	518.50	534.74

10. Preliminary neutron kinetics analyses

Because of the nature of the VCTR, a coupled system with a fast and thermal reactor, a question that arises is that of the adequacy of the use of the point kinetics approximation in transient calculations for accident scenarios. In order to answer this question, and investigate the effect of coupling on the neutron kinetics, a new code based on Avery's theory reported in Appendix A has been developed by G. Palmiotti.

More specifically, this new code solves the coupled equations (17a) and (17b) presented in Appendix A that in the case of the VCTR are limited to two reactors, and computes the time behavior of the power in the two regions (fast and thermal) of the system for any type of accident scenario. The code has the capability of introducing reactivity feedbacks due to temperature (e. g. Doppler, mechanical expansion, etc.) or insertion of negative reactivity (e. g. control rods). Six delayed neutron families are used. The two sets of β_{eff} (one for each region), the coupling coefficients, neutron prompt lifetimes, and lambdas for each delayed neutron families are gathered by the corresponding neutron transport SERPENT calculations. For describing the reactivity insertion of the accidents and the corresponding feedbacks, coupling coefficients, again provided by SERPENT, are used.

Among the reactivity coefficients that were calculated, the coolant void of the thermal zone in the Pu-LEU configuration generates a positive reactivity insertion; therefore, this case was chosen in order to investigate the time power behavior. Concerning the temperature reactivity feedbacks, only the Doppler coefficient was used (1.5 degree of increase in the fuel corresponding to 1% increase in power, see Table 9.3 in thermal analysis section). Moreover, the power increase is controlled via insertion of the safety rods. In summary these are the conditions of the computed accident scenario:

- Voiding of the thermal zone core (100% of sodium coolant) in 0.2 seconds (e. g. an air bubble traveling at 5 m/sec along the one meter height of the thermal core).
- Insertion of the safety rods, located in the intermediate zone between the fast and the thermal, starting after 0.2 seconds of the beginning of the voiding.
- Total duration of the investigated transient: 0.5 seconds.

Figure 10.1 shows the power behavior during the transient. The two regions (fast and thermal) powers are normalized to one. The total power is also normalized to one and it is the sum of the two separated powers. The total power behavior should be equivalent to that calculated by a point kinetic code with quantities (reactivity, β_{eff}, lambdas, etc.) averaged over the whole system. As it can be seen the power rises up to 0.2 seconds, where it reaches an increase of a factor of ~1.3, and then decreases to ~ 0.6 of the initial power at the end of the time period considered.

As it can be observed, there is no significant difference in the power behavior of the two zones, as well when compared to the total one (corresponding to point kinetics). This is confirmed by Table 10.1 where we show the relative power change at the end of the time period in the two zones. No significant differences can be detected between the two values of the fast and thermal region with respect to that of the total system. This behavior can be attributed to the strong coupling between the two regions. This, in turn, makes possible to perform transient studies using the point kinetics approximation. In Appendix B, a more thorough analysis of coupled system behavior, based on Avery's theory, supports this conclusion.

Table 10.1. Relative power values at 2 seconds after the beginning of the reactivity insertion, due to 100% coolant voiding in the thermal zone of the system.

Region	Relative power at 0.5 seconds
Fast	0.556
Thermal	0.568
Total	0.564

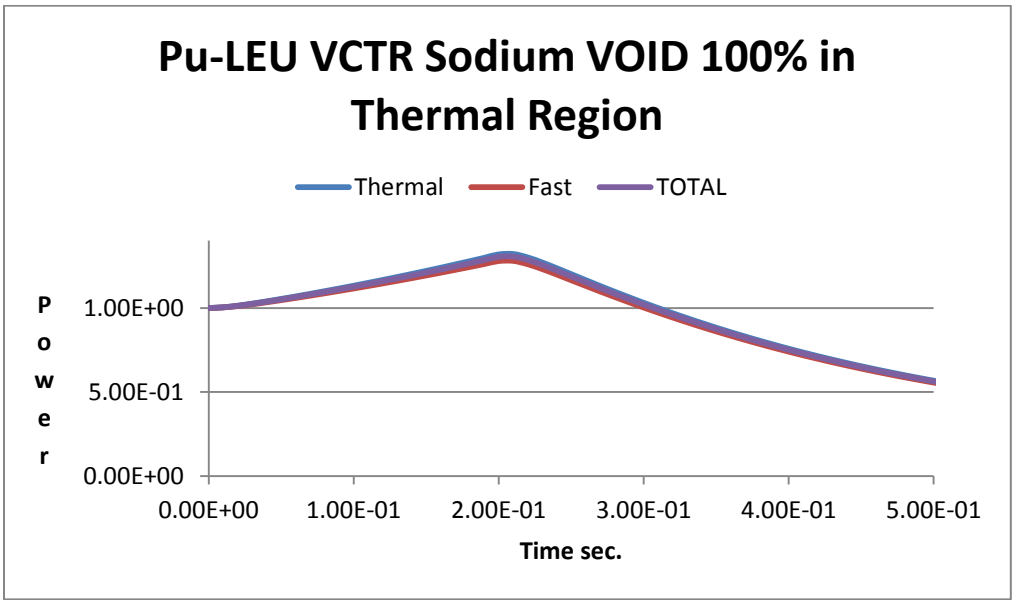

Figure 10.1. Time power behavior under insertion of reactivity due to 100% coolant voiding in the thermal zone of the system.

11. Systems considerations

Physical Design, Constraints and Challenges

The present VCTR design concept is a sodium-cooled loop reactor with primary coolant pumped from the reactor tank through intermediate heat exchanges heating the secondary coolant loops. Primary and secondary coolant pumps are located within the loops, outside the reactor tank. Fundamental to this basic design are several important considerations; reactor safety, experimental facility design requirements, and experimental facility access.

Reactor safety is clearly the principal requirement for the reactor design. As a loop reactor, the VCTR reactor tank design becomes an important consideration fundamental to safety performance. In addition, the reactor tank is the location for crucial fuel and experimental handling equipment operations and as such must meet a diverse set of functional requirements. The final sizing of the reactor tank volume will be performed in the near future, based on an optimization of safety, thermal hydraulic and experimental handling considerations.

The choice of a loop reactor was in part based on reactor operating floor access. This access is maximized in the loop configuration by locating the primary pumps in the primary coolant loops. Accordingly, the reactor operating floor is maintained uncluttered for experimental and fuel handling needs. In addition, this design consideration will provide operational efficiency through separation of maintenance and operational functions that compete for this limited floor space.

Some past test reactors have been built and placed into operation with difficult experimental access, intricate safety analysis requirements, and limited experimental data acquisition support. The challenge for a successful test reactor is to address appropriate issues in the design phase and get the details right while meeting a range of customer and user requirements. Although substantial efforts have been expended to date, the current design only considers possible customer requirements and generic capabilities. As such this is only a starting place, recognizing it is important not to be presumptuous. Experimental facility design requirements, established through interactions with identified and potential customers are an important component and will be formally solicited in the future.

It is important to point out the difficulty in designing experimental vehicles to meet customer requirements while controlling fabrication, routine safety analysis, and cost of operation. Current experimental vehicle designs have considered a number of potential capabilities including various irradiation vehicles from basic driver fuel hardware up to and including fueled experiments, with coolants not compatible with the reactor's sodium coolant. Coolants considered in addition to sodium include; heavy liquid metals (lead), lead-bismuth eutectic alloy, molten salts, pressurized water and gases. Also of high importance is the collection of high fidelity data within the irradiation vehicle.

Reactor access for the experimental vehicle is also of prime importance; appropriate reactor access goes hand-in-hand with affordability and operational considerations. Reactor access also addresses the preparation and loading of experimental vehicles, reactor ingress and egress, and post irradiation vehicle handling to support timely post irradiation preparations.

Summarizing, the current VCTR design has established feasibility from a physics perspective while a physical reactor and plant configuration has been conceptualized to support assumed experimental conditions and customer requirements. With the overarching goal of supporting the nuclear development community with a versatile test facility that meets their requirements now, in the near term and into the future.

Configuration

The configuration of the VCTR was focused by the decision to be a test reactor with experimental aspects taking the first priority after safety; thus the VCTR will not generate electrical power and the reactor oper-

ating floor should provide the maximum experimental access. The generation of electrical power, although considered, was eliminated due to potential conflicts with experimental program needs.

The VCTR design consists of a conventional sodium cooled-loop configuration, as are the majority of test reactors, providing a clear reactor top and unencumbered experimental access as a priority. The decision to use a large rector tank, i.e., sodium pool, without the primary coolant pumps and intermediate heat exchangers, is the basis of a clear reactor top, physically separating the maintenance functions from routine experimental and fuel handling operations.

The loop design may evolve to a larger reactor tank and thus an increased sodium inventory based primarily on safety considerations. The advantage of the additional capacity during thermal transients provides significant safety margin.

Current descriptive drawings of the VCTR are shown with the reactor tank containing necessary control and safety rod mechanisms, fuel and experimental handling capabilities. All other systems, i.e., primary and secondary coolant pumps, intermediate heat exchangers and sodium-to air heat exchanger, are located within the primary and secondary cooling loops.

Control

Reactivity control and neutronic shutdown are provided by conventional suspended mechanisms driven from the reactor operating floor. Control and shutdown capability will reside in a conventional rotating plug assembly allowing access to the core for fuel handling operations

Cooling Systems

The VCTR employs multiple loops for cooling; redundant electromagnetic primary coolant pumps are located on each on the reactor primary cooling loops external to the reactor tank. Secondary cooling loops utilize electromagnetic coolant pumps and heat is removed through redundant intermediate heat exchangers (sodium-to-sodium) followed by secondary cooling heat transfer to the atmosphere through multiple sodium-to-air heat exchangers.

Fuel and Experimental Assembly Handling

VCTR experimental irradiations are performed in several different irradiation vehicles; standard core assemblies, instrumented assemblies within standard core hardware, experimental loops within standard core hardware, and experiential loops requiring isolation from the reactor's sodium coolant which by their configuration require significant balance of plant connectivity.

The handling process for driver fuels, reflector assemblies and experimental assemblies using standard "core assembly hardware" are the same. The VCTR utilizes a system of three pantographic handling machines, three in-tank storage baskets, and two transfer ports. The juxtaposition of the transfer ports to the storage baskets support loading and removal operations of assemblies during reactor operation.

Fresh fuel and experimental assemblies are placed into a shielded transfer machine that interfaces with the sealed reactor tank. The assembly passes from the shielded transfer machine, through the reactor tank head via a transfer port into the reactor tank. Assemblies are transferred through the transfer port directly into a storage basket. Alternatively, the assembly can be handled by one of the pantographic core loading machines for placement in a storage basket, or conversely, the assembly can be transferred directly into the appropriate core location. Assemblies can be moved from one storage basket to another as needed.

Fueled or experimental assemblies are transferred out of the reactor tank by reversing this process. Irradiated assemblies will be removed from the reactor tank into the shielded transfer machine before placement into an inter-building cask. The inter-building cask is located below grade and within an airlock, providing reactor building atmosphere control, between the reactor and the collocated hot-cell facility.

As mentioned above, the VCTR has been designed to accommodate a number of different experimental configurations; configurations for the irradiation of fuels or materials that will accommodate a variety of coolants including: sodium, lead, lead-bismuth eutectic (LBE), high-pressure water and gas coolants with isolation from the reactor's primary coolant system. In addition, a hydraulic transfer system is planned for irradiations of limited volumes or specimens with short-term duration exposure requirements.

Experiments requiring isolation from the VCTR primary coolant will be performed within a closed loop consisting of a thimble that is suspended from the reactor-tank upper closure. Experimental access to a thimble will utilize a heavily shielded experiment handling cask serving as the loading and unloading interface between the hot cell facility and the reactor. Upon removal from the reactor, the experimental loop and or its contents are transfer to the collocated hot-cell facility, via the shielded experimental handling cask, for post irradiation examination preparation.

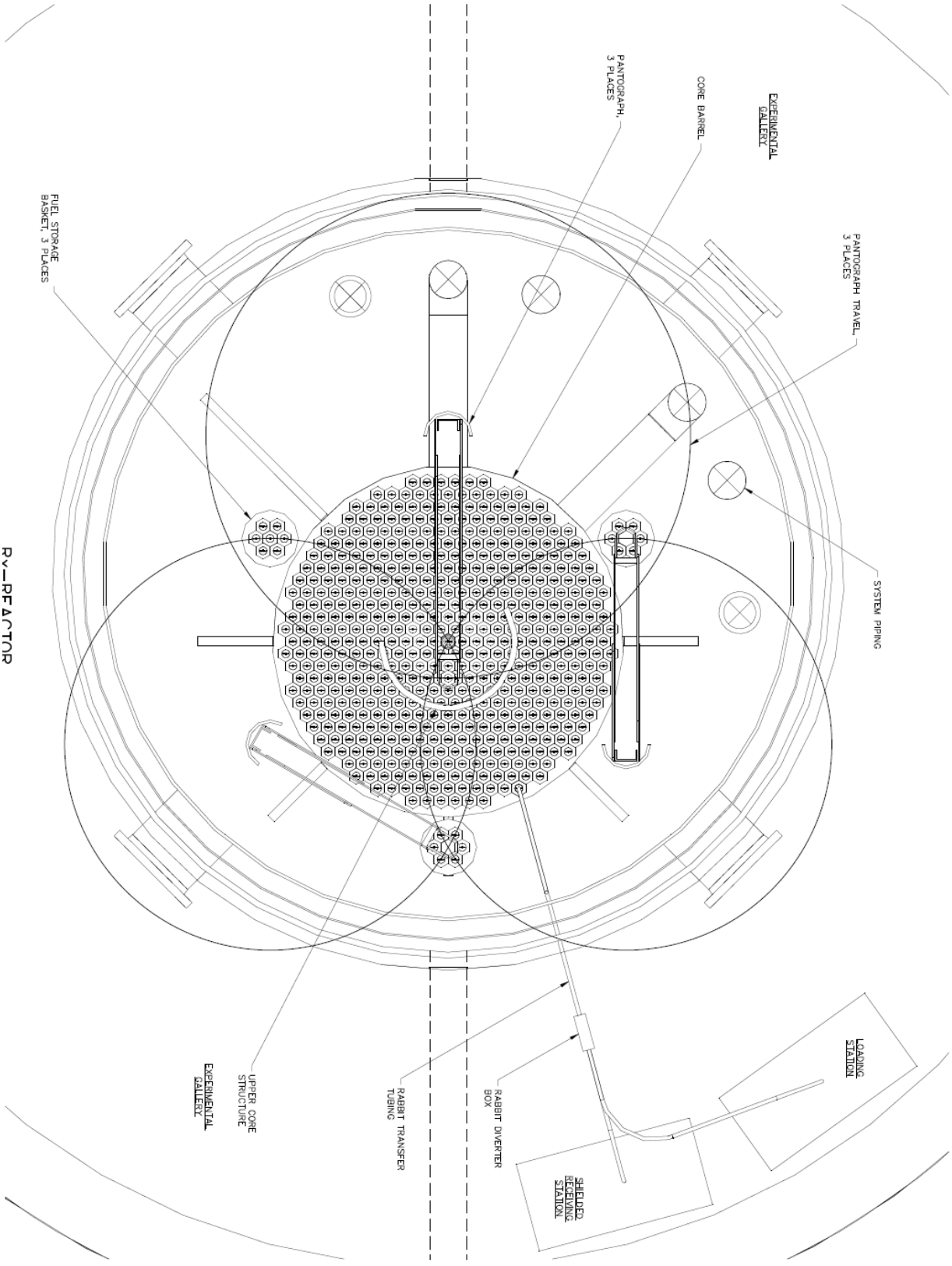

Figure 11.1. Cross-sectional view showing the reach of the three fuel handling machines and the three fuel storage baskets.

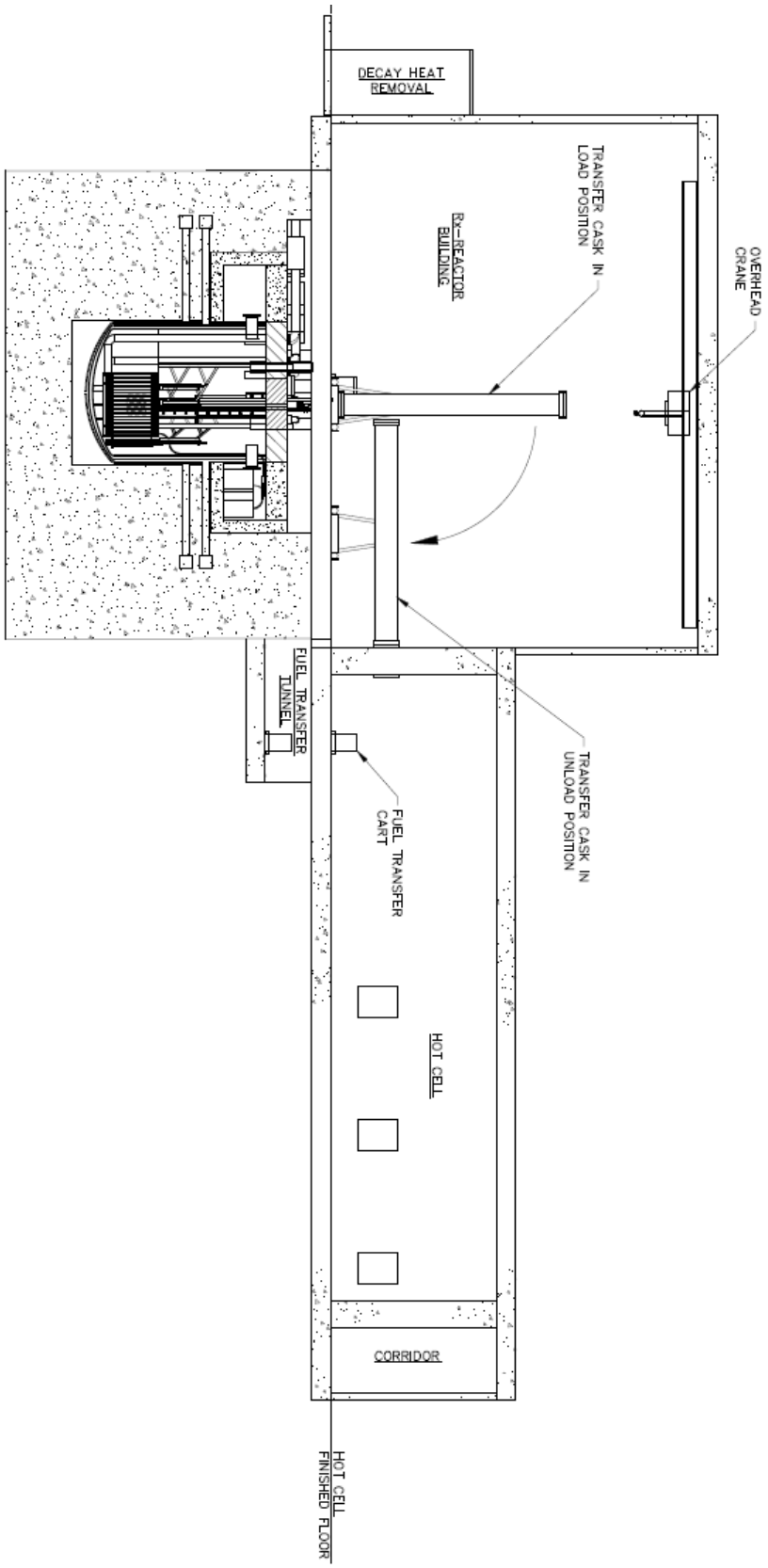

Figure 11.2. Cross-section of the VCTR reactor, reactor building and fuel handling interface with the post irradiation examination preparation facility

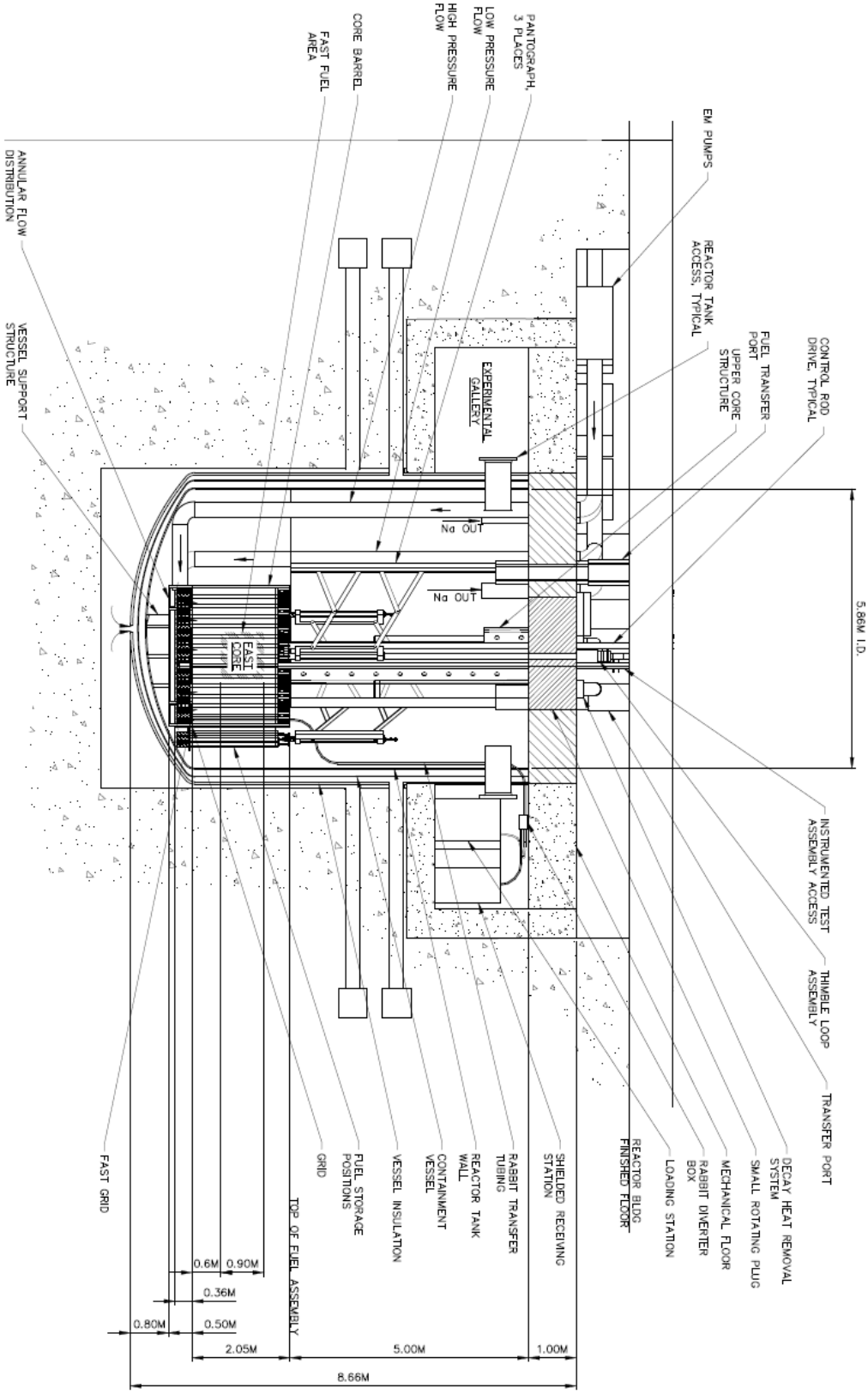

Figure 11.3. Cross-sectional view of the VCTR reactor and reactor tank.

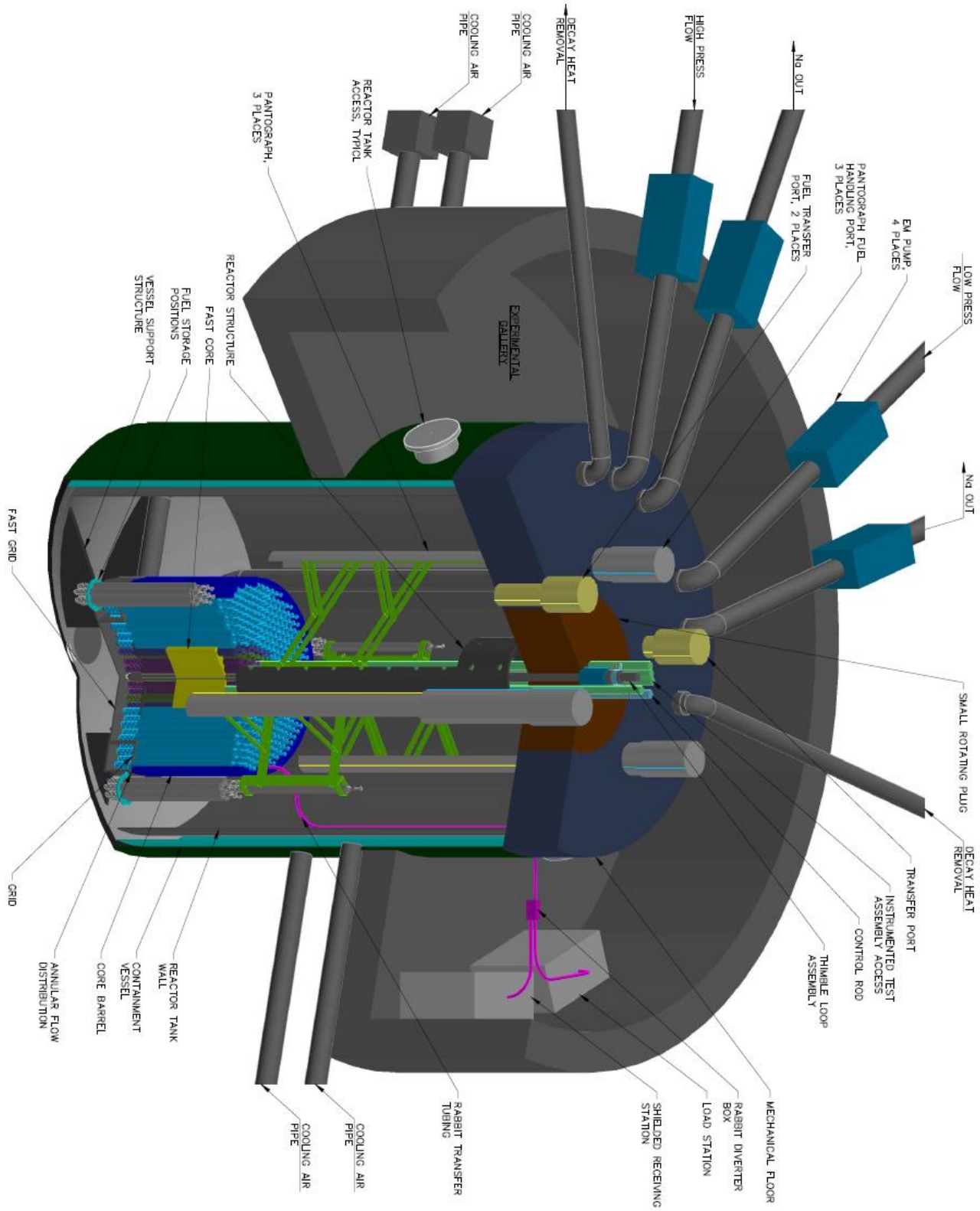

Figure 11.4. Isometric representation of the VCTR showing the operating floor and reactor tank facilities.

12. Safety considerations

The VCTR is a multiple-spectrum critical reactor with a fast-neutron spectrum central region surrounded by a thermal-neutron spectrum region. As with any reactor, the overall safety needs to be assured, and any specific safety issues identified that would need to be addressed by the design. This section discusses the current view on the safety of the VCTR and describes any special safety issues that could arise. Due to the preliminary nature of the concept, this discussion only provides an overview covering the major safety topics, and it is expected that more detailed safety analyses would be performed as the concept evolves into a design. Some factors that affect reactor safety are determined by the neutronic characteristics of the reactor core (including those affected by core structural characteristics), others are determined by the design of the reactor (including the coolant and heat-rejection systems), and others are determined by both. The operation of the reactor itself is discussed first, and then the implications of the planned experiments are covered.

Normal Operations

In order for the VCTR to be a viable concept, it must be possible to control the reactor as desired, resulting in predictable operation the reactor. While the remainder of the plant (e.g., coolant system, heat rejection capability, etc.) would be similar to other reactors and should not pose any issues, there are several factors concerning the reactor core that are important in determining whether a critical reactor can be successfully controlled and operated.

Delayed-Neutron Fraction

Delayed neutrons are essential for controlling a nuclear reactor and the amount of delayed neutrons is expressed by the delayed-neutron fraction. The delayed-neutron fraction must be sufficient to allow control of the fission process, and is determined by the isotopes undergoing fission, e.g., fission of plutonium-239 has a smaller delayed neutron fraction than fission of uranium-235. Experience has shown that fast reactors using either predominantly plutonium-239 or uranium-235 fission can be adequately controlled, indicating that the range of delayed neutron fraction represented by these isotopes should result in acceptable controllability of the reactor. For the VCTR, a plutonium-fueled design should have a delayed neutron fraction somewhere within the range of experience for fast reactors, which should indicate that control of the reactor is possible. The coupled thermal region should have a similar delayed-neutron fraction, and with the neutronic coupling of the two zones predominantly having the fast region providing neutrons to the thermal region resulting in the fast-neutron and thermal-neutron regions simultaneously responding to any changes in core reactivity, it should be possible to design the VCTR so that the delayed-neutron fraction would be acceptable.

Reactivity Balance

As with any reactor, core reactivity must be controllable for stable operation. The reactivity balance for fast neutron reactors can be expressed as the sum of the three coefficients below:

- *Power Coefficient*. The power coefficient is the change in core reactivity caused by a change in core power. It is essential for the power coefficient to be negative, i.e., to have a negative effect on core reactivity in response to a power increase. In fast reactors, the power coefficient is normally dependent on the Doppler coefficient of the fuel, which is negative for both oxide and metallic fuels. For the thermal zone, a similar situation would exist for the Doppler coefficient, leading to the conclusion that the VCTR should be able to be designed with an overall negative power coefficient.

- *Power-to-Flow Coefficient*. The power-to-flow coefficient is the change in core reactivity in response to a change in the core power-to-flow ratio, e.g. increasing power without increasing flow rate would increase the power-to-flow ratio. It is essential that the power-to-flow coefficient also be negative, that is, an increase in the core power-to-flow ratio would have a negative effect on the core reactivity, acting to mitigate the increase in core power. The power-to-flow coefficient is dependent on several reac-

tivity feedbacks, including fuel thermal expansion, cladding thermal expansion, coolant density, control rod driveline thermal expansion, and core radial expansion, the first four of which are inherently negative, but the core thermal expansion feedback can be positive or negative, depending on the design of the core restraint system. The core radial expansion coefficient can also be of larger magnitude than the others, and it is important to manage the sign and magnitude of this coefficient. By proper design of the core restraint system, such as using the "limited free-bow" approach demonstrated in FFTF, the coefficient can be reliably negative, at least for typical power-to-flow ratios used for startup and normal operations. For the VCTR, the presence of the outer thermal zone complicates the situation and the radial fuel worth gradient must be examined to ensure that any fuel displacement in the radial direction due to changes caused by changes in the power-to-flow ratio are in the direction of decreasing the fuel worth, which in turn provides negative feedback. At this time, there is no evidence that this condition can't be met with the VCTR.

- *Inlet Temperature Coefficient*. The inlet temperature coefficient is the change in core reactivity with a change in the core inlet temperature, and includes the same reactivity feedback coefficients as the power-to-flow coefficient, along with an additional coefficient corresponding to the change in reactivity due to a change in the grid plate temperature causing a change in the grid plate dimensions. Since this also affects the radial dimension of the core, the design of the core restraint system must also account for changes in grid plate dimensions. The considerations are the same as they are for the core radial expansion coefficient, and the design of the VCTR must take the grid plate effect into account.

Startup and Shutdown

Startup from hot standby must be done in a controllable manner using both power and flow until nominal operating conditions are attained. Previous experience with fast reactors shows that this is possible for a range of the parameters described above. Addition of the thermal zone around the fast reactor core in the VCTR is not anticipated to modify conditions sufficiently to prevent a similar startup procedure, as long as the design provisions mentioned above are adquately addressed. For the same reason it is also expected that controlled shutdown would similarly be achievable without difficulty. "Reactor trip" or "scram" is not usually included in this category since it is not considered to be part of normal operation.

Anticipated Operational Occurrences

These are events that are expected to occur at least once during the lifetime of the facility, such as a loss of offsite power, which corresponds to a probability of occurrence of greater than $1x10^{-2}$ per reactor-year, and according to the NRC for LWRs include but are not limited to loss of power to all recirculation pumps, tripping of the turbine generator set, isolation of the main condenser, and loss of all offsite power. Of most interest in this category of events from a safety perspective are the scrammed events, since reactor scram is a much more rapid shutdown of the reactor and may be accompanied by other aspects such as using natural circulation cooling of the core. From a neutronics perspective, the VCTR should respond to scram in a manner similar to other reactors since it is possible to have the scram system introduce sufficient negative reactivity to shut down the reactor, but the design must ensure that all characteristics provide an acceptable response, especially the ability of the flow to transition from forced cooling to natural circulation. Nothing has been identified for the VCTR that would prevent successful response to these events.

Accidents

Accidents are events that are not expected to occur during the lifetime of the plant, but are possible in principle. The design determines the possibility of the accident initiators and the probability of occurrence for any given accident initiator, with accidents of increasing consequences being designed to have progressively lower probability of occurrence.

Design-Basis Accidents. Design-basis accidents are postulated accidents that a nuclear facility must be designed and built to withstand without loss to the systems, structures, and components necessary to ensure public health and safety. The accident initiators typically have a probability of occurrence between $1x10^{-2}$ and $1x10^{-5}$ per reactor-year. Accidents in this category all tend to be protected events, e.g.,

scram system functions properly, so that the consequences are related to the resulting plant response after scram. Experience with both fast and thermal reactors indicate that acceptable response can be designed into the plant so that the regulatory requirements are met for this category of accidents. There are no indications that the coupled core of the VCTR would present any new challenges in this area in principle, but if certain design choices were changed, such as the use of separate coolant loops for the fast and thermal section of the reactor core, the change could raise safety issues. The current design does not appear to have made any such choices, and and as a result, it is expected that the VCTR could be designed to have acceptable response to this category of accidents.

Beyond Design-Basis Accidents (a.k.a. Design Extension Conditions). According to the NRC today, this term "beyond design-basis accidents" is used as a technical way to discuss accident sequences that are possible but were not fully considered in the design process because they were judged to be too unlikely. (In that sense, they are considered beyond the scope of the design-basis accidents that a nuclear facility must be designed and built to withstand, but the plant needs to have an acceptable response to these events as well. They are analyzed "best-estimate" rather than with "conservative" estimates.) Since the regulatory process strives to be as thorough as possible, "beyond design-basis" accident sequences are analyzed to fully understand the capability of a design. Accidents under design-extension conditions have a probability of occurrence in the range of $1x10^{-5}$ to $1x10^{-7}$. Both thermal and fast reactors have been designed and constructed that have acceptable responses to this category of accidents. Again, the use of a coupled core in the VCTR does not in principle appear to introduce any new issues with respect to this class of accidents, and the current design does not appear to have any design choices that would introduce new issues. As mentioned earlier, in case of an unprotected prompt reactivity excursion starting at low operating power (e.g. accident due to rapid withdrawal of control rods), the peak power is inversely proportional to the prompt-neutron lifetime. Consequently, the peak pressures and accelerations, caused by material expansion, would be much smaller in the VCTR than in a more standard fast test reactor because the prompt neutron lifetimes are, respectively, about 100 microseconds and 0.5 microsecond. Note that, with regard to reactivity accidents, a recent IAEA document [**16**] reports that "Research reactors are sensitive to this kind of incident, due to the large number of manipulations which are done, often with fuel elements with a high enrichment. In research reactors, the insertion or withdrawal of irradiation samples at power can also add significant amounts of reactivity." This particular aspect will need to be quantified further as part of the safety evaluation.

Experimental Loops

The addition of experimental loops in several locations in the core of the VCTR introduces potential safety issues that are not encountered with a typical reactor, mainly due to the characteristics of the loops, containing the fuel being tested and a coolant loop that is separate from that of the VCTR. It is envisioned that some loops may be designed for testing fuels at high pressure with water as the coolant, or at high pressure with gas coolant. Both of these place high pressure vapor sources in the core region, and the design must accommodate the failure of the pressure boundaries without propagating into the reactor core assemblies. Otherwise, one introduces new accidents not typically encountered with fast reactors, such as the introduction of vapor into the core (which can have a large positive reactivity effect), along with a possible exothermic chemical reaction in the case of a steam/sodium reaction. All test loops need to be evaluated for characteristics that may pose a risk to the reactor. Accidents concerning the test loops will need to be considered as part of licensing use of these test loops in the reactor (which can be a separate licensing activity), regardless of the authorizing agency, but these are specific to the test loop, not to the reactor in general.

Test Assemblies

The VCTR is also envisioned to allow insertion of test fuel assemblies in place of the standard core assemblies. Since the test assemblies will share the same coolant loop and plant control / protection system, there is the potential for such test assemblies to introduce new safety issues for operation of VCTR, and these would need to be evaluated for each test assembly, especially if there is a risk of fuel failure or other similar significant failures in the test assembly. Also, since test assemblies will likely require additional instrumentation, these additions would also need to be evaluated for any potential safety impact.

13. Conclusions

A new irradiation test reactor is a costly investment that will operate for several decades and the initial specifications are crucial to ensure the relevance of such a facility in the long run. This new test reactor should be highly reconfigurable and allow operation as a fast test reactor or a thermal test reactor or a coupled fast-thermal test reactor. This report presents the on-going effort at Idaho National Laboratory (INL) to design a versatile coupled test reactor (VCTR) that could fulfill the R&D needs requiring high fast neutron fluxes but also high thermal neutron fluxes in configurations that could not be met in current thermal neutron test reactors such as ATR. In this work, a coupled reactor is defined as a reactor with two distinct spectral zones (Fast and Thermal), which are neutronically coupled to each other; some neutrons born in zone F cause fission in zone T and vice-versa. Only fast neutrons are allowed to go from one zone to the other. A neutron filter keeps thermal neutrons from diffusing into the fast zone.

A distinction can be made depending on the main purpose of using fuel assemblies with some level of neutron moderation (thermal zone) together with fuel assemblies with as little moderation as possible (fast zone). It can be used mainly to minimize the core power and fissile inventory—in this case the configuration is said to be boosted—or it can be used mainly to provide additional control of the irradiation conditions in the thermal zone. The extent to which both objectives can be reached at the same time depends on other constraints such as the total power of the reactor.

The present VCTR design concept is a sodium-cooled loop reactor with primary coolant pumped from the reactor tank through intermediate heat exchanges heating the secondary coolant loops. Primary and secondary coolant pumps are located within the loops, outside the reactor tank. Fundamental to this basic design are several important considerations; reactor safety, experimental facility design requirements, and experimental facility access. Coupled cores, if properly designed, do not appear to introduce new safety issues; no particular issues are anticipated for control either.

The 270 MW boosted core design presented in this report is far from optimized and will continue to evolve, but, even though more analyses are necessary to quantify it further, it shows that an LEU boosted core design would be smaller than a more standard LEU fast test reactor design. Significant cost savings are anticipated by operating a test reactor with a smaller thermal power. Significant simplifications of the logistic are also anticipated if the test reactor does not have to rely on the use of a (weapons-grade) plutonium-based fuel. The peak fast flux (above 0.1 MeV) at the center of the fast zone, where a test loop could be located, is currently about 3.5×10^{15} n/s.cm^2 and work is underway to increase this value further. The unperturbed peak thermal flux (below 0.625 eV) in the graphite reflector is about 10^{15} n/s.cm^2, about twice what is currently achievable in ATR flux traps.

As mentioned above, the VCTR design is only in a very preliminary stage and is still subject to modifications, some of which could possibly adversely lower the core reactivity. If necessary, some plutonium could also be used in conjunction with LEU as a way to increase the reactivity, and, consequently, the cycle length and fuel burnup. The addition of 1 percent of plutonium to the fuel would require no more than approximately 13 kg of plutonium per year. At this rate—even if a few percent of plutonium were used for the fuel fabrication—there is enough plutonium present at INL to provide an additional source of fissile material for several decades of operation without having to rely on an external source of weapons-grade plutonium.

Of course, if available, weapons-grade plutonium could also be used and a detailed cost-benefit analysis regarding the use of LEU versus plutonium should be carried out. The use of plutonium in the fast zone would provide more flexibility in fuel assembly design than when low enriched uranium is used because, the reactivity worth of plutonium being higher than that of uranium-235, the designer has more degrees of freedom to work with; in particular it could provide additional control of the irradiation conditions in the thermal zone.

14. References

[1] JP Dupuy et al. "Jules Horowitz Reactor; General Design, main design options resulting from safety options, technical performances and operating constraints" Proc. TRTR2005/IGORR-10 Joint Meeting, Gaithersburg, Maryland, USA (Sept. 2005); See also http://www-cadarache.cea.fr/rjh/news.html

[2] Yu.G. Dragunov et al, "MBIR Multipurpose Fast Reactor", Atomic Energy, Vol 113, No.1, November 2012; See also World Nuclear News article "Russia's MBIR gets construction license", http://www.world-nuclear-news.org/NN-Russias-MBIR-gets-construction-licence-15051501.html

[3] R. Avery, "Coupled fast-thermal power breeder reactor", US Patent No: 2,992,982, Jul 18, 1961 (filed Dec 10, 1957)

[4] K. Dietze, "Integral Test of Neutron Data and Comparison of Codes by Re-Analysis of the SEG and STEK Experiments", *JEFF Working Group Meeting,* Aix-en-Provence, May 16-18, 2001, JEFF/DOC-861

[5] W. Marth, "The History of the Construction and Operation of the German KNK II Fast Breeder Power Plant", Kf K-5456, November 1994

[6] J. Leppanen, "Serpent – a Continuous-energy Monte Carlo Reactor Physics Burnup Calculation Code – User's Manual", VTT Technical Research Centre of Finland, June 18, 2015

[7] C. B. Davis, Applicability of RELAP5-3D for Thermal-Hydraulic Analyses of a Sodium-Cooled Actinide Burner Test Reactor, INL/EXT-06-11518, July 2006.

[8] M. Memmot, J. Buonjiorno, and P. Hejzlar, "On the Use of RELAP5-3D as a Subchannel Analysis Code," Nuclear Science and Engineering, Volume 240, Number 4, pp. 807-815, April 2010.

[9] A. Del Nevo and E. Martelli, "Validation of a Three-Dimensional Model of EBR-II and Assessment of RELAP5-3D Based on SHRT-17 Test," Nuclear Technology, Volume 193, Number 1, pp. 1-14, January 2016.

[10] W. F. G. van Rooijen and H. Mochizuki, "Analysis of the EBR-II SHRT-45R Unprotected Loss of Flow Experiment with ERANOS and RELAP," Science and Technology of Nuclear Installations, 2015.

[11] C. B. Davis, "Thermal-hydraulic Analyses of Transients in an Actinide-burner Reactor Cooled by Forced Convection of Lead-bismuth," Nuclear Engineering and Design 335, pp. 149-160, 2003.

[12] P. Hejzlar, and C. B. Davis, "Performance of the Lead-Alloy-Cooled Reactor Concept Balanced for Actinide Burning and Electricity Production," Nuclear Technology, Vol. 147, No. 3, pp. 344-367, September 2004.

[13] Takafumi Aoyama, Takashi Sekine, Shiro Tabuchi, "Characterization of neutron field in the experimental fast reactor JOYO for fuel and structural material irradiation test", Nuclear Engineering and Design 228 (2004) 21–34

[14] Shigetaka Maeda , Masaya Yamamoto , Tomonori Soga , Takashi Sekine, Takafumi Aoyama, "Core Modification to Improve Irradiation Efficiency of the Experimental Fast Reactor Joyo", Journal of Nuclear Science and Technology, 48:4, 693-700 (2011)

[15] International Atomic Energy Agency, "Fast Reactor Database, 2006 Update", IAEA-TECDOC-1531, December 2006.

[16] International Atomic Energy Agency, "Operating Experience from Events Reported to the IAEA Incident Reporting System for Research Reactors", IAEA-TECDOC-1762, March 2015

APPENDIX A

R. Avery, "Theory of Coupled Reactors", Proc. Int. Conf. *Second United Nations International Conference on the Peaceful Uses of Atomic Energy,* United Nations, Geneva 1958

Theory of Coupled Reactors

By R. Avery*

COUPLED SYSTEM PARAMETERS

The general formulation of the reactor equations, as given by the time, space, and energy dependent Boltzmann equation, may be applied, formally at least, to any system however complicated. To say then that a system consists of coupled reactors, an irrelevant concept in the general formulation, is a statement only of how one wishes to consider the system, and implies, of course, that it is believed advantageous to do so.

The individual reactors of the coupled system are arbitrarily defined by any prescription which specifies the reactor in which each fission neutron is emitted. The term "coupled" is taken to mean that in each of the reactors some of the fission neutrons are emitted in fissions induced by neutrons born in other reactors. A fission neutron source may be associated with each of the reactors. The total source is the sum of the individual reactor sources. Further, each of the reactor sources gives rise to a next generation source in other reactors.

The formalism that is developed treats the system in terms of integral parameters which explicitly characterize the individual reactors and the coupling between them. k_{ij} is defined as the expectation value that a fission neutron in reactor j gives rise to a next generation fission neutron in reactor i, and l_{ij} is defined as the average prompt neutron lifetime for the process. k_{ij} for $i \neq j$ is a measure of the cross coupling from reactor j to reactor i, and in general $k_{ij} \neq k_{ji}$.

The quantity $1 - k_{ii}$ occurs frequently and it is therefore convenient to define $\Delta_i \equiv 1 - k_{ii}$. Δ_i is a measure of the subcriticality of reactor i without the contribution of the other reactors.

S_i is defined as the total fission neutron source in reactor i, and S_{ij} is defined as the total fission neutron source in reactor i which results from fissions caused by neutrons which originate in reactor j. We then have

$$S_i = \sum_{j=1}^{N} S_{ij} \tag{1}$$

where N is the number of reactors in the system.

The definitions of the various integral parameters, k_{ij}, l_{ij}, S_i and S_{ij} are applicable for both the steady state and time dependent situation. Their definition requires some sort of averaging procedure or weighting procedure in integration. A detailed discussion of this is deferred until the section "Correlation with General Formulation."

* Argonne National Laboratory, Lemont, Illinois, U.S.A.

REACTIVITY CONSIDERATIONS

The critical condition that the k_{ij} must satisfy is considered first for the case of two coupled reactors. From the basic definitions of the k_{ij}, S_{ij}, and S_i, the following steady state ratios hold:

$$\frac{S_{11}}{S_1} = k_{11}; \quad \frac{S_{12}}{S_2} = k_{12}; \quad \frac{S_{21}}{S_1} = k_{21}; \quad \frac{S_{22}}{S_2} = k_{22}. \tag{2}$$

Also, from Eq. (1),

$$S_{11} + S_{12} = S_1 \tag{3a}$$
$$S_{21} + S_{22} = S_2. \tag{3b}$$

Substitution of Eqs. (2) into Eqs. (3) gives,

$$k_{11}S_1 + k_{12}S_2 = S_1 \tag{4a}$$
$$k_{21}S_1 + k_{22}S_2 = S_2. \tag{4b}$$

The condition for criticality is given by the condition that a self-consistent solution exists to Eqs. (4), and further that this solution corresponds to non-negative values for the S_i. This latter condition is necessary to rule out cases where one of the reactors is supercritical on its own. The criticality condition for the two reactor case is thus,

$$\begin{vmatrix} (k_{11} - 1) & k_{12} \\ k_{21} & (k_{22} - 1) \end{vmatrix} = 0, \tag{5}$$

which may also be given as,

$$k_{12}k_{21} = \Delta_1\Delta_2. \tag{6}$$

The above relationships are all valid even if the cross coupling in one or both directions vanishes. If the coupling to one of the reactors from the other vanishes, then it must be critical on its own. The coupling in the other direction and the reactivity of the other reactor may be any value providing the other reactor is subcritical.

After having satisfied the criticality condition, one can solve for the relative values of the S_i. For the two reactor case this gives

$$\frac{S_1}{S_2} = \frac{k_{12}}{\Delta_1} = \frac{\Delta_2}{k_{21}}. \tag{7}$$

Even if the cross coupling vanishes in one direction, the power ratio given in Eq. (7) is still valid, though

one of the two expressions will be indeterminate. If both cross couplings vanish, then both expressions for the power ratios are indeterminate, and of course any power ratio can in fact exist between the two independent critical reactors.

We now consider the reactivity of a non-critical system. We do this in the usual way in terms of the fictitious value of the number of neutrons per fission, ν_c, needed to maintain criticality. At non-criticality $\nu \neq \nu_c$ and the fission neutron source in one generation will reproduce itself in the next generation with a magnitude which differs by a factor k, where $k = \nu/\nu_c$. For small deviations from criticality, $k_{ex} \approx \rho$, where $k_{ex} = k - 1$, and the reactivity, $\rho = -\delta\nu/\nu = (\nu - \nu_c)/\nu$.

For the two reactor case,

$$\begin{pmatrix} k_{11} & k_{12} \\ k_{21} & k_{22} \end{pmatrix} \begin{pmatrix} S_1 \\ S_2 \end{pmatrix} = k \begin{pmatrix} S_1 \\ S_2 \end{pmatrix}. \tag{8}$$

Using $k = 1 + k_{ex}$ we obtain from Eq. (8) the following expression for k_{ex}:

$$\Delta_1\Delta_2 + k_{ex}(\Delta_1 + \Delta_2) + k_{ex}^2 = k_{12}k_{21}. \tag{9}$$

This expression is valid without restriction even if one or both of the reactors are supercritical by themselves. For the case where the reactivity is very small compared to the subcriticality of each of the reactors, we can neglect k_{ex}^2 in Eq. (9) and obtain the approximate expression

$$k_{ex} \approx \rho \approx \frac{k_{12}k_{21} - \Delta_1\Delta_2}{\Delta_1 + \Delta_2}. \tag{10}$$

A more useful approximate expression for the reactivity is obtained by expressing it in terms of the deviations from the critical values,

$$\rho \approx \frac{\Delta_1\Delta_2}{\Delta_1 + \Delta_2}\left(-\frac{\delta\Delta_1}{\Delta_1} - \frac{\delta\Delta_2}{\Delta_2} + \frac{\delta k_{12}}{k_{12}} + \frac{\delta k_{21}}{k_{21}}\right). \tag{11}$$

A straightforward generalization to N reactors gives

$$\begin{pmatrix} k_{11} & k_{12} & \cdots & k_{1N} \\ k_{21} & k_{22} & \cdots & k_{2N} \\ \cdot & \cdot & & \cdot \\ \cdot & \cdot & & \cdot \\ \cdot & \cdot & & \cdot \\ k_{N1} & k_{N2} & & k_{NN} \end{pmatrix} \begin{pmatrix} S_1 \\ S_2 \\ \cdot \\ \cdot \\ \cdot \\ S_N \end{pmatrix} = k \begin{pmatrix} S_1 \\ S_2 \\ \cdot \\ \cdot \\ \cdot \\ S_N \end{pmatrix} \tag{12}$$

which defines the reactivity of a non-critical system and which gives for the criticality condition

$$|k_{ij} - \delta_{ij}| = 0, \tag{13}$$

where δ_{ij} is the Kronecker delta function. The power ratios can be determined from Eq. (12) and at criticality the solution must be such that no negative values for the S_i result.

We now consider a general hypothetical problem. Assume in the two reactor case that in each of the reactors the value of ν is changed by amount $\delta\nu_1$ in reactor 1 and $\delta\nu_2$ in reactor 2. With the corresponding changes in the k_{ij}, it can be shown from Eq. (11) that:

$$\rho \approx \frac{\dfrac{1}{\Delta_1}}{\dfrac{1}{\Delta_1} + \dfrac{1}{\Delta_2}}\frac{\delta\nu_1}{\nu_1} + \frac{\dfrac{1}{\Delta_2}}{\dfrac{1}{\Delta_1} + \dfrac{1}{\Delta_2}}\frac{\delta\nu_2}{\nu_2}. \tag{14}$$

We can generalize the above result to N coupled reactors and find that:

$$\rho \approx \sum_{i=1}^{N} \alpha_i \frac{\delta\nu_i}{\nu_i}, \tag{15}$$

where

$$\alpha_i = \frac{1}{\Delta_i}\Big/\sum_{j=1}^{N}\frac{1}{\Delta_j}. \tag{16}$$

The previous considerations lead to the concept of division of reactivity. α_i, the fraction of reactivity in reactor i, is defined as the ratio of the over-all reactivity to $\delta\nu_i/\nu_i$, where the reactivity results from the change of ν_i to $\nu_i + \delta\nu_i$.

KINETICS EQUATIONS

In terms of the previously defined integral parameters the following equations describe the kinetic behavior of the coupled system:

$$\ell_{jk}\frac{dS_{jk}}{dt} = k_{jk}(1-\beta)\sum_{m=1}^{N} S_{km} - S_{jk} + k_{jk}\sum_{i=1}^{D}\lambda_i C_{ki} \tag{17a}$$

$$\frac{dC_{ki}}{dt} = \beta_i \sum_{m=1}^{N} S_{km} - \lambda_i C_{ki}. \tag{17b}$$

In Eqs. (17), β is the total effective delayed neutron fraction, β_i and λ_i are the effective delayed neutron fraction and decay constant respectively, of the ith delayed neutron precursor, D is the total number of such delayed neutron precursor types, and C_{ki} is a properly weighted measure of the number of delayed neutron emitters of the ith type in reactor k.

For simplicity we have assumed not the most general characteristics for the delayed neutrons, but that the β, β_i, λ_i are all independent of the reactor and also that the k_{jk} and ℓ_{jk} for delayed neutrons are the same as for prompt neutrons. If these assumptions are not made, the only consequence is that there are additional variables and the notation is more involved, but no basic complication results.

Before further discussing the form of the kinetics equations, we introduce the redundant variables N_{jk}, defined by:

$$S_{jk} \equiv \frac{N_{jk}}{\ell_{jk}}. \tag{18}$$

We do this only to aid in the exposition, since now the equations will be put in a form that is close in analogy to the usual kinetics equations. Using N_{jk}, instead of S_{jk}, Eqs. (17) become

$$\frac{dN_{jk}}{dt} = k_{jk}(1-\beta)\sum_{m=1}^{N}\frac{N_{km}}{\ell_{km}} - \frac{N_{jk}}{\ell_{jk}} + k_{jk}\sum_{i=1}^{D}\lambda_i C_{ki} \tag{19a}$$

$$\frac{dC_{ki}}{dt} = \beta_i \sum_{m=1}^{N}\frac{N_{km}}{\ell_{km}} - \lambda_i C_{ki}. \tag{19b}$$

N_{jk} may be thought of as a quantity similar to a neutron density. It serves as a measure of the number of neutrons, properly weighted, in the system which were born in reactor k and are destined to produce next generation neutrons in reactor j.

The physical arguments leading to Eqs. (19) are the usual ones for kinetics equations. dN_{jk}/dt is given by the difference in production and loss rates for N_{jk} type neutrons. The production rate consists of two terms; production by prompt neutron emission and production by delayed neutron emission.

$$S_k = \sum_{m=1}^{N} S_{km} = \sum_{m=1}^{N} \frac{N_{km}}{\ell_{km}}$$

represents the total number of source neutrons in reactor k of which $(1-\beta)S_k$ are prompt. Therefore, $k_{jk}(1-\beta)S_k$, the first term on the right hand side of Eq. (19a) is the production rate of the N_{jk} type neutrons by prompt neutron emission. βS_k represents the total number of delayed source neutrons in reactor k, and of these $\beta_i S_k$ are of the ith precursor type, so that this term represents the production rate term in Eq. (19b) for C_{ki}. The ith precursor decays with a decay constant λ_i, so that $\lambda_i C_{ki}$ represents the loss rate for C_{ki}. The difference between production and loss rates for C_{ki} gives dC_{ki}/dt from which Eq. (19b) follows. The total number of delayed source neutrons in reactor k is $\sum_{i=1}^{D} \lambda_i C_{ki}$, so that $k_{jk} \sum_{i=1}^{D} \lambda_i C_{ki}$, the last term on the right hand side of Eq. (19a), is the production rate of N_{jk} type neutrons by delayed neutron emission. Finally N_{jk}/ℓ_{jk} represents the loss rate of N_{jk} type neutrons from which Eq. (19a) follows.

The reason the coupled equations are as complicated as they are, and the reason it was necessary to introduce the partial sources, S_{jk}, or the related N_{jk}, results from the fact that there is no correlation between the branching ratios, k_{jk}, that a neutron born in reactor k may take in giving rise to fission neutrons in the various final reactors, $j = 1, 2, \ldots N$, and the lifetime, ℓ_{jk}, that it takes to do so. If the various k_{jk} were inversely proportional to the ℓ_{jk}, as is usually the case when there are competing modes of decay, then a more compact description of the neutron kinetic behavior would have been possible.

For the two reactor case, Eqs. (19) become,

$$\frac{dN_{11}}{dt} = k_{11}(1-\beta)\left(\frac{N_{11}}{\ell_{11}} + \frac{N_{12}}{\ell_{12}}\right) - \frac{N_{11}}{\ell_{11}} + k_{11}\sum_{i=1}^{D}\lambda_i C_{1i} \tag{20a}$$

$$\frac{dN_{21}}{dt} = k_{21}(1-\beta)\left(\frac{N_{11}}{\ell_{11}} + \frac{N_{12}}{\ell_{12}}\right) - \frac{N_{21}}{\ell_{21}} + k_{21}\sum_{i=1}^{D}\lambda_i C_{1i} \tag{20b}$$

$$\frac{dN_{12}}{dt} = k_{12}(1-\beta)\left(\frac{N_{21}}{\ell_{21}} + \frac{N_{22}}{\ell_{22}}\right) - \frac{N_{12}}{\ell_{12}} + k_{12}\sum_{i=1}^{D}\lambda_i C_{2i} \tag{20c}$$

$$\frac{dN_{22}}{dt} = k_{22}(1-\beta)\left(\frac{N_{21}}{\ell_{21}} + \frac{N_{22}}{\ell_{22}}\right) - \frac{N_{22}}{\ell_{22}} + k_{22}\sum_{i=1}^{D}\lambda_i C_{2i} \tag{20d}$$

$$\frac{dC_{1i}}{dt} = \beta_i\left(\frac{N_{11}}{\ell_{11}} + \frac{N_{12}}{\ell_{12}}\right) - \lambda_i C_{1i} \tag{20e}$$

$$\frac{dC_{2i}}{dt} = \beta_i\left(\frac{N_{21}}{\ell_{21}} + \frac{N_{22}}{\ell_{22}}\right) - \lambda_i C_{2i}. \tag{20f}$$

The usual procedure for solving the coupled kinetics equations is to assume that the k_{jk}, but not the ℓ_{jk}, may be time dependent, and then to solve for the time dependence of the N_{jk} and C_{ki}. We could assume that the ℓ_{jk} are also time dependent, but just as one ordinarily does not assume in the usual kinetics equations that the prompt lifetime, l, is time dependent, so we will usually assume constant ℓ_{jk}. The time dependence of the k_{jk} can be given explicitly and/or as some function or functional of the various N_{jk}. The latter is fully analogous to the dependence of k on n in the usual kinetics equations. We expect that in the coupled case the equations will generally have to be solved numerically, although we are able to obtain some results from analytic considerations.

ADJOINT FORMULATION

We now consider the equations adjoint to the coupled kinetics equations. For simplicity we assume no delayed neutrons. For the uses that we will make of the adjoint formulation, this assumption will in no way limit us. For the case of all neutrons prompt we obtain for the coupled kinetics equation.

$$\frac{dN_{jk}}{dt} = k_{jk}\sum_{m=1}^{N}\frac{N_{km}}{\ell_{km}} - \frac{N_{jk}}{\ell_{jk}}. \tag{21}$$

The equations adjoint to Eq. (21) are:

$$\frac{dN_{jk}^*}{dt} = \sum_{m=1}^{N} k_{mj}\frac{N_{mj}^*}{\ell_{jk}} - \frac{N_{jk}^*}{\ell_{jk}}. \tag{22}$$

For the two reactor case Eq. (22) becomes:

$$\frac{dN_{11}^*}{dt} = k_{11}\frac{N_{11}^*}{\ell_{11}} + k_{21}\frac{N_{21}^*}{\ell_{11}} - \frac{N_{11}^*}{\ell_{11}} \tag{23a}$$

$$\frac{dN_{21}^*}{dt} = k_{12}\frac{N_{12}^*}{\ell_{21}} + k_{22}\frac{N_{22}^*}{\ell_{21}} - \frac{N_{21}^*}{\ell_{21}} \tag{23b}$$

$$\frac{dN_{12}^*}{dt} = k_{11}\frac{N_{11}^*}{\ell_{12}} + k_{21}\frac{N_{21}^*}{\ell_{12}} - \frac{N_{12}^*}{\ell_{12}} \tag{23c}$$

$$\frac{dN_{22}^*}{dt} = k_{12}\frac{N_{12}^*}{\ell_{22}} + k_{22}\frac{N_{22}^*}{\ell_{22}} - \frac{N_{22}^*}{\ell_{22}}. \tag{23d}$$

We can solve for the ratios of the steady state values of the N_{jk}^* in this case and obtain:

$$N_{11}^* = N_{12}^* \equiv N_1^* \tag{24a}$$

$$N_{21}^* = N_{22}^* \equiv N_2^* \tag{24b}$$

and, in general:

$$N_{jk}^* = N_{j1}^* \equiv N_j^*$$

$$N_1^* = \frac{k_{21}}{\Delta_1}N_2^* = \frac{\Delta_2}{k_{12}}N_2^* \tag{24c}$$

$$\frac{N_{11}^*S_{11} + N_{12}^*S_{12}}{N_{21}^*S_{21} + N_{22}^*S_{22}} = \frac{N_1^*S_1}{N_2^*S_2} = \frac{\Delta_2}{\Delta_1}. \tag{24d}$$

α_i, given by Eq. (16), reduces for the two reactor case to:

$$\alpha_i = \frac{1}{\Delta_i}\Big/\left(\frac{1}{\Delta_1}+\frac{1}{\Delta_2}\right). \tag{25}$$

α_i may then also be expressed by:

$$\alpha_i = \frac{N_i^* S_i}{N_1^* S_1 + N_2^* S_2}. \tag{26}$$

From the definition of α_i an alternate expression for its value can be obtained. We consider the usual perturbation formula where only the value of ν is perturbed. The resulting reactivity change is given by

$$\rho \approx \frac{\int \chi(v')\phi^*(r,v')\dfrac{\delta\nu}{\nu}\nu\sigma_f(r,v)\phi(r,v)\,dr\,dv\,dv'}{\int \chi(v')\phi^*(r,v')\nu\sigma_f(r,v)\phi(r,v)\,dr\,dv\,dv'},$$

where $\chi(v')$ is the normalized fission spectrum, $\phi(r,v)$ is the neutron flux, $\phi^*(r,v')$ is the adjoint function, and $\sigma_f(r,v)$ is the macroscopic fission cross section.

Assume that $\delta\nu/\nu$ is non-vanishing only over reactor i, and that it is there constant, so that it can be taken outside the integral. Therefore,

$$\rho \approx \frac{\delta\nu_i}{\nu_i}\frac{\int_{\text{reactor } i}\chi(v')\phi^*(r,v')\nu\sigma_f(r,v)\phi(r,v)\,dr\,dv\,dv'}{\int_{\text{entire system}}\chi(v')\phi^*(r,v')\nu\sigma_f(r,v)\phi(r,v)\,dr\,dv\,dv'}.$$

We see from Eqs. (15) and (26) that α_i is given by the coefficient of $\delta\nu_i/\nu_i$ in Eq. (26), and is equal to the fraction of the importance production rate due to all fission source neutrons born in reactor i. By comparison with Eq. (26) the interpretation of N_i^* as the average importance of a fission neutron born in reactor i follows.

The rate at which importance is removed from or born into the j, kth region, and also the entire system, may be given in terms of the S_j, S_{jk}, and N_k^*.

Rate at which importance removed from j, kth region

$$= N_{jk}^* S_{jk} = N_j^* S_{jk}. \tag{27}$$

Rate at which importance removed from entire system

$$= \sum_{j,k} N_{jk}^* S_{jk} = \sum_j N_j^* S_j. \tag{28}$$

Rate at which importance born into j, kth region

$$= k_{jk} N_{jk}^* S_k = k_{jk} N_j^* S_k. \tag{29}$$

Rate at which importance born into entire system

$$= \sum_{j,k} k_{jk} N_j^* S_k. \tag{30}$$

Using the steady state ratios at criticality it can easily be shown that values from Eqs. (27) and (28) are identical to those of Eqs. (29) and (30); i.e. at steady state the ratio of the rate of production of importance to the rate of removal of importance is unity.

The amount of importance in the j, kth region; i.e. the total amount of importance carried by all the neutrons in the system at any time which were born in reactor k and which are going to cause fissions in reactor j, is obtained from the product of the rate at which importance is removed from (or born into) the j, kth reactor and the lifetime for neutrons in the j, kth region. We then have

Amount of importance in j, kth region:

$$= N_j^* S_{jk} \ell_{jk} = N_j^* N_{jk}. \tag{31}$$

Amount of importance in entire system:

$$= \sum_{j,k} N_j^* N_{jk}. \tag{32}$$

We now develop a perturbation formula which relates the change in reactivity with a change from the critical values of the various k_{ij}. We have already obtained this result from previous considerations. The result is rederived as a means of illustration of the significance of the adjoint formulation. We assume that the k_{ij} are perturbed by an amount δk_{ij} and that the steady state is maintained by means of a fictitious change in ν of amount $\delta\nu$, where $\delta\nu/\nu = -\rho$. As a consequence of these perturbations the N_{jk} are themselves perturbed by an amount δN_{jk}. The resulting steady state equations are,

$$(k_{jk}+\delta k_{jk})(1-\rho)\sum_{m=1}^{N}\frac{(N_{km}+\delta N_{km})}{\ell_{km}} - \frac{(N_{jk}+\delta N_{jk})}{\ell_{jk}} = 0. \tag{33}$$

The unperturbed adjoint steady state equations are:

$$\sum_{m=1}^{N} k_{mj}\frac{N_{mj}^*}{\ell_{jk}} - \frac{N_{jk}^*}{\ell_{jk}} = 0. \tag{34}$$

We now apply the usual techniques of perturbation theory. We multiply the j, kth real perturbed equation by N_{jk}^* and sum over all j, k. From this we subtract the sum over all j, k of the product of the j, kth unperturbed adjoint equation and $(N_{jk}+\delta N_{jk})$, yielding:

$$\sum_{j,k} N_{jk}^*\left\{(k_{jk}+\delta k_{jk})(1-\rho)\sum_{m=1}^{N}\frac{(N_{km}+\delta N_{km})}{\ell_{km}} - \frac{(N_{jk}+\delta N_{jk})}{\ell_{jk}}\right\} - \sum_{j,k}(N_{jk}+\delta N_{jk})\left\{\sum_{m=1}^{N} k_{mj}\frac{N_{mj}^*}{\ell_{jk}} - \frac{N_{jk}^*}{\ell_{jk}}\right\} = 0.$$

The zero order terms; i.e. terms not involving any δ terms, cancel out because of the steady state condition of the unperturbed system. We ignore all terms higher than the first order. For the first order terms all terms involving δN_{jk} cancel out identically. We then obtain:

$$\rho = \frac{\sum_{j,k}\delta k_{jk} N_{jk}^* \sum_{m=1}^{N}\dfrac{N_{km}}{\ell_{km}}}{\sum_{j,k} k_{jk} N_{jk}^* \sum_{m=1}^{N}\dfrac{N_{km}}{\ell_{km}}} = \frac{\sum_{j,k}\delta k_{jk} N_j^* S_k}{\sum_{j,k} k_{jk} N_j^* S_k}. \tag{35}$$

For the two reactor case this becomes:

$$\rho = \frac{\sum_{m=1,2}\left[\delta k_{m1}N_{m1}^*\left(\frac{N_{11}}{\ell_{11}}+\frac{N_{12}}{\ell_{12}}\right)+\delta k_{m2}N_{m2}^*\left(\frac{N_{21}}{\ell_{21}}+\frac{N_{22}}{\ell_{22}}\right)\right]}{\sum_{m=1,2}\left[k_{m1}N_{m1}^*\left(\frac{N_{11}}{\ell_{11}}+\frac{N_{12}}{\ell_{12}}\right)+k_{m2}N_{m2}^*\left(\frac{N_{21}}{\ell_{21}}+\frac{N_{22}}{\ell_{22}}\right)\right]}, \tag{36}$$

which on substitution of the steady state ratios reduces to the result obtained previously in Eq. (11).

NEUTRON LIFETIME

The neutron lifetime, ℓ, serves as a measure of the average time between successive fission events caused by prompt neutrons. It is defined[1] as the ratio of the total neutron importance in the system to the rate at which importance is removed and in terms of the coupling parameters is given by:

$$\ell = \frac{\sum_{j,k} N_{jk}^* N_{jk}}{\sum_{j,k} N_{jk}^* S_{jk}} = \frac{\sum_{j,k} N_{jk}^* S_{jk}\ell_{jk}}{\sum_{j,k} N_{jk}^* S_{jk}}. \tag{37}$$

Since the relative steady state values of the various $N_{jk}^*\, S_{jk}$ do not involve the ℓ_{jk}, Eq. (37) gives the neutron lifetime as a linear combination of the partial lifetimes.

For the two reactor case the lifetime, ℓ, as given by Eq. (37) and the previously obtained steady state ratios, becomes:

$$\ell = \frac{\Delta_2 k_{11}}{\Delta_1+\Delta_2}\ell_{11} + \frac{\Delta_1 k_{22}}{\Delta_1+\Delta_2}\ell_{22} + \frac{\Delta_1\Delta_2}{\Delta_1+\Delta_2}(\ell_{12}+\ell_{21}). \tag{38}$$

It is clear from the definition of the lifetime that it is not the average time between fissions, since there is a non-constant weighting factor attached to intervals between fissions which depends on the importance and thus on location of the fission events. We can explicitly demonstrate this by giving the value for the average time between fissions for the two reactor case. For this average the weighting factor for ℓ_{jk} is:

$$S_{jk}/\sum_{j,k} S_{jk}$$

which then gives for the average time between fissions, $\bar{\ell}$,

$$\bar{\ell} = \frac{\Delta_2 k_{11}}{\Delta_2+k_{21}}\ell_{11} + \frac{\Delta_1\Delta_2}{\Delta_1+k_{12}}\ell_{21} + \frac{\Delta_1\Delta_2}{\Delta_2+k_{21}}\ell_{12} + \frac{\Delta_1 k_{22}}{\Delta_1+k_{12}}\ell_{22}. \tag{39}$$

In the expression for the lifetime in the two reactor case, Eq. (38), it may be seen that the contributions of the two cross lifetimes, ℓ_{12} and ℓ_{21} enter with the same weighting factor even though there are in general a different number of fissions associated with each lifetime, as may be seen from Eq. (39). This is a consequence of the fact that the relative importance for each type event is such as to maintain an equal total importance production for neutrons going from reactor 1 to 2 as for neutrons going from reactor 2 to 1.

An alternative definition of the neutron lifetime, but which is equivalent to the ratio of total importance to importance rate removal, considers an infinitely small perturbation in the value of ν of amount $\delta\nu$. Assuming all neutrons are prompt, the system will asymptotically approach an exponential time behavior, $e^{\omega t}$. The neutron lifetime is then defined by:

$$\lim_{\delta\nu,\omega\to 0}(\ell) = \left|\frac{1}{\omega}\cdot\frac{\delta\nu}{\nu}\right| \tag{40}$$

The definition of Eq. (40) can be used as the basis for another derivation for the expression for the neutron lifetime in the coupled formalism.

We use a method analogous to that ordinarily used to evaluate the perturbation theory expression for the lifetime in the usual kinetics formulation. Two separate eigenvalue problems are considered. The first, already considered, has as the eigenvalue the number of neutrons emitted per fission. One perturbs the system, i.e. the values of the k_{ij}, and determines the fictitious change in ν, $\delta\nu$, necessary to maintain criticality. The reactivity, $\rho = -\delta\nu/\nu$, corresponding to the perturbation is thus determined. The result of this analysis is given by Eq. (35). The other eigenvalue problem which we now consider deals with a fixed value of ν and considers the time constant, ω, corresponding to an exponential time behavior, $e^{\omega t}$, as the eigenvalue. The system is perturbed again by changing the values of the k_{ij}, and the change in ω is determined. The expression for ω contains quantities that can be recognized as the reactivity from the first eigenvalue problem. The lifetime, ℓ, is then determined by the relation, $\ell = \rho/\omega$. Proceeding, the perturbed kinetics equations with the time constant as the eigenvalue are:

$$(k_{jk}+\delta k_{jk})\sum_{m=1}^{N}\frac{(N_{km}+\delta N_{km})}{\ell_{km}} - \frac{(N_{jk}+\delta N_{jk})}{\ell_{jk}} = \omega(N_{jk}+\delta N_{jk}). \tag{41}$$

We consider along with Eq. (41) the unperturbed adjoint steady state equations, Eq. (34), and then form the usual combination of:

$$\sum_{j,k} N_{jk}^*\left\{(k_{jk}+\delta k_{jk})\sum_{m=1}^{N}\frac{(N_{km}+\delta N_{km})}{\ell_{km}} - \frac{(N_{jk}+\delta N_{jk})}{\ell_{jk}} - \omega(N_{jk}+\delta N_{jk})\right\} - \sum_{j,k}(N_{jk}+\delta N_{jk})\left\{\sum_{m=1}^{N}\frac{k_{mj}N_{mj}^*}{\ell_{jk}} - \frac{N_{jk}^*}{\ell_{jk}}\right\} = 0.$$

The zero order terms cancel out and we ignore higher order terms. The first order terms involving the δN_{jk} cancel out. We obtain:

$$\omega = \frac{\sum_{j,k}\delta k_{jk}N_{jk}^*\sum_{m=1}^{N}\frac{N_{km}}{\ell_{km}}}{\sum_{j,k}N_{jk}^*N_{jk}},$$

which along with Eq. (35) gives

$$l = \frac{\rho}{\omega} = \frac{\sum_{j,k} N_{jk}^* N_{jk}}{\sum_{j,k} k_{jk} N_{jk}^* \sum_{m=1}^{N} \frac{N_{km}}{l_{km}}} = \frac{\sum_{j,k} N_j^* S_{jk} l_{jk}}{\sum_{j,k} k_{jk} N_j^* S_k}. \quad (42)$$

The expression for the lifetime in Eq. (42) is consistent with that of Eq. (37), since at criticality the rate of production of importance, the denominator in Eq. (42), and the rate of removal of importance, the denominator in Eq. (37), are equal.

INHOUR EQUATION

We consider the problem of obtaining for the two reactor case the equivalent of the inhour equation, i.e. the equation relating the possible time constants with the parameters characterizing the system. We assume exponential solutions:

$$N_{jk}(t) = N_{jk}^0 e^{\omega t}; \; C_{ji} = C_{ji}^0 e^{\omega t}$$

and substitute into Eqs. (20). The condition that the determinant of the matrix of coefficients vanish yields after some algebra:

$$\left(\Delta_1 + \omega l_{11} + \omega k_{11} \sum_{i=1}^{D} \frac{\beta_i}{\omega + \lambda_i}\right) \times \left(\Delta_2 + \omega l_{22} + \omega k_{22} \sum_{i=1}^{D} \frac{\beta_i}{\omega + \lambda_i}\right)(1 + \omega l_{12})(1 + \omega l_{21}) = k_{12} k_{21} (1 + \omega l_{11})(1 + \omega l_{22}) \left(1 - \omega \sum_{i=1}^{D} \frac{\beta_i}{\omega + \lambda_i}\right)^2, \quad (43)$$

which is the desired equation.

If we assume that $\omega l \ll \Delta_1, \Delta_2$, i.e. take the limit for very long periods, so that terms of the order of ωl or higher can be neglected, the results yield the correct value of the neutron lifetime. In this approximation Eq. (43) reduces to:

$$\omega \left[\frac{\Delta_2 k_{11}}{\Delta_1 + \Delta_2} l_{11} + \frac{\Delta_1 k_{22}}{\Delta_1 + \Delta_2} l_{22} + \frac{\Delta_1 \Delta_2}{\Delta_1 + \Delta_2}(l_{12} + l_{21}) + \sum_{i=1}^{D} \frac{\beta_i}{\lambda_i} + 2\rho \sum_{i=1}^{D} \frac{\beta_i}{\lambda_i}\right] = \frac{k_{12} k_{21} - \Delta_1 \Delta_2}{\Delta_1 + \Delta_2}. \quad (44)$$

When the assumptions of this derivation are satisfied,

$$\frac{k_{12} k_{21} - \Delta_1 \Delta_2}{\Delta_1 + \Delta_2} \approx \rho.$$

Neglecting the higher order last term in the brackets on the left hand side of Eq. (44) we obtain:

$$\omega \left(l + \sum_{i=1}^{D} \frac{\beta_i}{\lambda_i}\right) \approx \rho, \quad (45)$$

where l has the same form as in Eq. (38). The relation of Eq. (45) is, of course, the one expected for very small reactivities.

PROMPT JUMP

The prompt jumps in neutron densities under step changes in the coupling parameters, k_{ij}, can be studied analytically with the aid of the coupled kinetics equations. We consider the situation when the step change in reactivity does not exceed the amount required to go prompt critical and determine the source strength in each region a short time after the change is made. By a short time one means a time that is short compared to the delayed neutron periods, but long compared to the lifetime of a prompt neutron chain. If we define S_1^0 and S_2^0 as the initial values of S_1 and S_2, and S_1^F and S_2^F as the values after the prompt jump, then

$$S_1^F = \frac{k_{11}\beta S_1^0 + k_{12}[(1-\beta) S_2^F + \beta S_2^0]}{1 - k_{11}(1-\beta)} \quad (46a)$$

$$S_2^F = \frac{k_{21}[(1-\beta) S_1^F + \beta S_1^0] + k_{22}\beta S_2^0}{1 - k_{22}(1-\beta)}, \quad (46b)$$

where all the k_{ij} are the values after the step change and where,

$$\beta S_1^0 = \sum_{i=1}^{D} \lambda_i C_{1i}^0$$

$$\beta S_2^0 = \sum_{i=1}^{D} \lambda_i C_{2i}^0$$

can be evaluated from the initial values of the k_{ij}.

The arguments leading to these expressions are similar to those that can be used in connection with the prompt jump in the normal kinetics equations; i.e. that the fission neutron level is determined by the product of the number of delayed neutrons coming into the system and the prompt multiplication. In the coupled case the argument is generalized in the following manner. The fission neutron level in each reactor is given by the product of the number of neutrons coming into the reactor, either as delays originating in the reactor or as neutrons originating in the other reactor, and the prompt multiplication of the reactor. The assumption in all cases, i.e. the normal or the coupled case, is that the rate of delayed neutrons emitted is unchanged immediately after the step change. We can solve for the unknowns S_1^F, S_2^F from Eqs. (46). S_1^F and S_2^F can be divided into the partial sources S_{jk}^F,

$$S_{11}^F = \frac{k_{11}\beta S_1^0 + k_{11}(1-\beta)k_{12}[(1-\beta) S_2^F + \beta S_2^0]}{1 - k_{11}(1-\beta)} \quad (47a)$$

$$S_{21}^F = k_{21}[(1-\beta) S_1^F + \beta S_1^0] \quad (47b)$$

$$S_{12}^F = k_{12}[(1-\beta) S_2^F + \beta S_2^0] \quad (47c)$$

$$S_{22}^F = \frac{k_{22}(1-\beta)k_{21}[(1-\beta) S_1^F + \beta S_1^0] + k_{22}\beta S_2^0}{1 - k_{22}(1-\beta)}. \quad (47d)$$

CORRELATION WITH GENERAL FORMULATION

We now consider the correlation of the coupled formalism that has been developed with a general formulation of the reactor equations. In so doing, we determine the exact definitions of the various coupling parameters and how to explicitly evaluate them.

We first consider the steady state. In the general formulation we make use of the following quantities:

$\phi(r, v)$, the neutron flux as a function of position and velocity

$\phi^*(r, v)$, the function adjoint to the neutron flux (the adjoint flux)

$\nu\sigma_f(r, v)$, the product of the average number of neutrons emitted per fission and the macroscopic fission cross section (the product may be a function of position and of incoming neutron velocity)

$[\nu\sigma_f(r, v)]_j$, the part of $\nu\sigma_f(r, v)$ which prescribes the reactor j; and $\sum_j [\nu\sigma_f(r, v)]_j = \nu\sigma_f(r, v)$

$\chi(v)$, the fission spectrum; $\int \chi(v)\, dv = 1$

$\phi_j(r, v)$, for this quantity we make use of concepts related to the source iterative technique[2] of solution of the reactor equations. To determine the critical flux distribution one uses as the fission neutron source:

$$\chi(v)\int \nu\sigma_f(r, v')\phi(r, v')\, dv'.$$

One then determines the resulting neutron flux, treating fission events as removal events. After the flux has been completely determined one can then evaluate a new fission neutron source, which after the method has converged and the correct flux obtained, agrees with the initial fission neutron source. $\phi_j(r, v)$ is the resultant single iteration flux from a source:

$$\chi(v)\int [\nu\sigma_f(r, v')]_j \phi(r, v')\, dv'.$$

It is the part of the steady state flux that results from neutrons born in reactor j; and

$$\sum_j \phi_j(r, v) = \phi(r, v).$$

$\phi_j^*(r, v)$, a similar iterative technique, can be used to solve the adjoint problem. In this case the "source" is

$$\nu\sigma_f(r, v)\int \chi(v')\phi^*(r, v')\, dv'.$$

$\phi_j^*(r, v)$ is the resultant adjoint flux from a "source":

$$[\nu\sigma_f(r, v)]_j \int \chi(v')\phi^*(r, v')\, dv';$$

and

$$\sum_j \phi_j^*(r, v) = \phi^*(r, v).$$

As is well known $\phi^*(r, v)$ can be interpreted as the importance function; i.e. $\phi^*(r, v)$ serves as a measure of the extent to which a neutron at r with velocity v ultimately contributes to the maintenance of the chain reaction. $\phi_j^*(r, v)$ can be interpreted as the part of the importance function which is contributed by neutrons which will cause their next fission in reactor j.

In correlating the coupling parameters with the general quantities just defined, we begin with the definition that S_j is equal to the total fission neutron source in reactor j,

$$S_j = \int [\nu\sigma_f(r, v)]_j \phi(r, v)\, dr\, dv. \tag{48}$$

Analogously we have for the delayed neutron emitters,

$$C_{ji} = \frac{\beta_i}{\lambda_i}\int [\nu\sigma_f(r, v)]_j \phi(r, v)\, dr\, dv. \tag{49}$$

In dividing the total source in reactor j into the partial sources, S_{jk}, arising from neutrons originating in the various other reactors, we do so by taking the fraction of the total importance arising from fission neutrons in the reactor j which results from neutrons from the various other reactors. Thus,

$$S_{jk} = \frac{\int [\nu\sigma_f(r, v)]_j \phi(r, v)\, dr\, dv}{\int \chi(v')\phi^*(r, v')[\nu\sigma_f(r, v)]_j \phi(r, v)\, dr\, dv\, dv'} \times \int \chi(v')\phi^*(r, v')[\nu\sigma_f(r, v)]_j \phi_k(r, v)\, dr\, dv\, dv' \tag{50}$$

Because of the definition used in Eq. (50) we are able to assign the same average importance to all the partial sources in reactor j; i.e. $N_{jk}^* = N_{jl}^* \equiv N_j^*$.

At the steady state

$$k_{jk} = \frac{S_{jk}}{S_k}$$

so that

$$k_{jk} = \frac{\int [\nu\sigma_f(r, v)]_j \phi(r, v)\, dr\, dv}{\int [\nu\sigma_f(r, v)]_k \phi(r, v)\, dr\, dv} \times \frac{\int \chi(v')\phi^*(r, v')[\nu\sigma_f(r, v)]_j \phi_k(r, v)\, dr\, dv\, dv'}{\int \chi(v')\phi^*(r, v')[\nu\sigma_f(r, v)]_j \phi(r, v)\, dr\, dv\, dv'}. \tag{51}$$

$N_j^* S_{jk}$ is to be interpreted as the total importance of the fission neutrons in reactor j which result from neutrons born in reactor k. Therefore,

$$N_j^* S_{jk} = \int \chi(v')\phi^*(r, v')[\nu\sigma_f(r, v)]_j \phi_k(r, v)\, dr\, dv\, dv'$$

and thus:

$$N_j^* = \frac{\int \chi(v')\phi^*(r, v')[\nu\sigma_f(r, v)]_j \phi(r, v)\, dr\, dv\, dv'}{\int [\nu\sigma_f(r, v)]_j \phi(r, v)\, dr\, dv\, dv'}. \tag{52}$$

We see that N_j^* just represent the average importance of all fission neutrons born in reactor j.

The over-all neutron lifetime, ℓ, is given by the well known expression:

$$\ell = \frac{\int \frac{\phi^*(r, v)\phi(r, v)\, dr\, dv}{v}}{\int \chi(v')\phi^*(r, v')\nu\sigma_f(r, v)\phi(r, v)\, dr\, dv\, dv'},$$

which may also be written in the form:

$$\ell = \frac{\sum_{j,k} \int \frac{\phi_j^*(r, v)\phi_k(r, v)\, dr\, dv}{v}}{\int \chi(v')\phi^*(r, v')\nu\sigma_f(r, v)\phi(r, v)\, dr\, dv\, dv'} \tag{53}$$

In terms of the coupled formalism, ℓ is given by Eq. (37). The denominators of Eqs. (37) and (53) are equivalent. Recalling the interpretations of $\phi_i^*(r, v)$

and $\phi_k(r, v)$, we associate each of the j, k terms in the numerator of Eq. (53) with the corresponding j, k term of the numerator of Eq. (37) and obtain:

$$\ell_{jk} = \frac{\int \frac{\phi_j^*(r,v)\phi_k(r,v)\,dr\,dv}{v}}{\int \chi(v')\phi^+(r,v')[\nu\sigma_f(r,v)]_j \phi_k(r,v)\,dr\,dv\,dv'} \tag{54}$$

from which it also follows that:

$$N_{jk} = S_{jk}\ell_{jk}$$

$$= \frac{\int[\nu\sigma_f(r,v)]_j\phi(r,v)\,dr\,dv \int \frac{\phi_j^*(r,v)\phi_k(r,v)\,dr\,dv}{v}}{\int \chi(v')\phi^+(r,v')[\nu\sigma_f(r,v)]_j \phi(r,v)\,dr\,dv\,dv'}. \tag{55}$$

In order to determine the k_{jk} for a non-critical configuration, we first consider the steady state problem with a fictitious value of number of neutrons emitted per fission, ν_c. We use the fluxes as they result from the problem, evaluate the k_{jk} in the usual manner and obtain the desired results by multiplying the values by ν/ν_c.

APPLICATION TO FAST-THERMAL SYSTEM

The preceding formalism was developed in connection with a study of coupled fast-thermal systems, particularly as they may be applied to nuclear power breeders.[3, 4] We use this system to give some illustrations of the application of the formalism.

Useful qualitative considerations may be made from the power ratio given by Eq. (7). In the fast-thermal system one wants the ratio of fast to slow power, S_F/S_S, large for breeding gain purposes and one also wants the subcriticality of the fast part, Δ_F, substantial for safety purposes. It is clear from consideration of

$$\frac{S_F}{S_S} = \frac{k_{FS}}{\Delta_F}$$

that it is important to make k_{FS} as large as possible in order to satisfy both objectives. In practice, obtaining a large value of k_{FS} will have to be achieved subject to a competing requirement of maintaining a barrier between the fast and thermal parts which keeps the neutron spectrum high in the fast part.

As an illustration of the use of Eq. (11) we consider a change in the thermal utilization of the thermal reactor and we wish to determine the resultant change of reactivity. In the change of thermal utilization only Δ_S and k_{SF} are changed to first order,

$$\frac{\delta k_{SS}}{k_{SS}} = \frac{\delta k_{SF}}{k_{SF}} = \frac{\delta\eta_t}{\eta_t}.$$

Therefore,

$$\rho \approx \frac{\Delta_F\Delta_S}{\Delta_F + \Delta_S}\left(-\frac{\delta\Delta_S}{\Delta_S} + \frac{\delta k_{SF}}{k_{SF}}\right)$$

$$\rho \approx \frac{\frac{1}{\Delta_S}}{\frac{1}{\Delta_S} + \frac{1}{\Delta_F}}\frac{\delta\eta_t}{\eta_t}. \tag{56}$$

If we apply Eq. (38) to the fast-thermal system we obtain

$$\ell = \frac{\Delta_S k_{FF}}{\Delta_F + \Delta_S}\ell_{FF} + \frac{\Delta_F k_{SS}}{\Delta_F + \Delta_S}\ell_{SS} + \frac{\Delta_F\Delta_S}{\Delta_F + \Delta_S}(\ell_{SF} + \ell_{FS}). \tag{57}$$

In this system ℓ_{FF} and ℓ_{FS} are very short since they are associated with neutrons that cause fissions while still fast. ℓ_{SS} and ℓ_{SF} are orders of magnitude longer since they are associated with neutrons that slow down and diffuse about before causing thermal fissions. As a first approximation for determining the neutron lifetime in a fast-thermal system, we may neglect ℓ_{FF} and ℓ_{FS} with respect to ℓ_{SS} and ℓ_{SF} and set $\ell_{SS} = \ell_{SF} = \ell_S$. We then obtain:

$$\ell \approx \frac{\frac{1}{\Delta_S}}{\frac{1}{\Delta_S} + \frac{1}{\Delta_F}}\ell_S; \tag{58}$$

i.e. the neutron lifetime is approximately equal to the product of the fraction of reactivity in the thermal reactor and the slow neutron lifetime.

The expression for the neutron lifetime given previously refers to the value at the steady state. However, the more important quantity is the neutron lifetime during a transient. In the usual system it is invariably assumed, and usually with much validity, that the neutron lifetime is a constant of the system and therefore does not change during a transient. That this might not be the case in a fast-thermal system can be seen from the following example. Assume that reactivity is added linearly to the fast part (k_{FF} is increased linearly in time) so that the system finally becomes critical on fast neutrons alone. Then during the transient the neutron lifetime changes drastically. We can see from this type of consideration that there is a possibility for much different kinetic behavior in, for example, two systems which have the same neutron lifetime, but in one case $k_{SS} = k_{FF} = 0.995$ and in the other $k_{SS} = k_{FF} = 0.8$. In both cases the over-all lifetime is half the thermal lifetime, but in the first case it might be very easy for the system to outrun the thermal neutrons and take off on a period characteristic of fast systems. Thus, in some cases we have to study the kinetic behavior of the system on the basis of the coupled kinetics equations and not be able to deduce the kinetic behavior from the steady state neutron lifetime and the solutions of the ordinary kinetics equations.

The study on the basis of the coupled formalism yields a method of studying the kinetic behavior of coupled systems in a realistic manner which circumvents the difficulties encountered in the above example and which, while it is somewhat more complicated than the usual kinetics formulation, is far less involved than a general space and time dependent formulation.

In the fast-thermal system, under some conditions

we can make approximations which simplify the coupled kinetics equations considerably. We first assume ℓ_{FF}, $\ell_{FS} \ll \ell_{SF}$, ℓ_{SS}. We further restrict ourselves to those transients for which the system is never critical on fast neutrons alone. Under these assumptions we can, with considerable validity, set:

$$\frac{dN_{FF}}{dt} = 0, \text{ equivalent to setting } \ell_{FF} = 0$$

and

$$\frac{dN_{FS}}{dt} = 0, \text{ equivalent to setting } \ell_{FS} = 0.$$

We shall refer to the resulting equations as the reduced set of coupled kinetic equations.

The assumptions are very similar to that often used in the ordinary kinetics equations when one sets $dn/dt = 0$ in the range below prompt critical. This is equivalent to setting the prompt neutron lifetime equal to zero. In the ordinary kinetics equations this corresponds to saying that when a delayed neutron enters the system, the resulting prompt burst of fissions occurs instantaneously. In the fast-thermal case, the approximation corresponds to saying that when a neutron is emitted either from thermal fission or from a delayed emitter any resulting fast fissions (i.e. fissions occurring in the chain until a thermal fission breaks the branch of the chain) occur instantaneously. Clearly, in the stated ranges, the approximations are quite valid for both the coupled or ordinary kinetic equations.

With the notation of $1 \leftrightarrow F$ and $2 \leftrightarrow S$, the reduced coupled kinetics equations take the form

$$[1 - k_{11}(1-\beta)]\frac{N_{11}}{\ell_{11}} = k_{11}(1-\beta)\frac{N_{12}}{\ell_{12}} + k_{11}\sum_{i=1}^{D}\lambda_i C_{1i} \tag{59}$$

which results from $\frac{dN_{11}}{dt} = 0$, and

$$\frac{N_{12}}{\ell_{12}} = k_{12}(1-\beta)\left(\frac{N_{21}}{\ell_{21}} + \frac{N_{22}}{\ell_{22}}\right) + k_{12}\sum_{i=1}^{D}\lambda_i C_{2i} \tag{60}$$

from $\frac{dN_{12}}{dt} = 0$.

Substituting Eq. (60) into Eq. (59) we obtain:

$$\frac{N_{11}}{\ell_{11}} = \frac{k_{11}(1-\beta)\left[k_{12}(1-\beta)\left(\frac{N_{21}}{\ell_{21}} + \frac{N_{22}}{\ell_{22}}\right) + k_{12}\sum_{i=1}^{D}\lambda_i C_{2i}\right] + k_{11}\sum_{i=1}^{D}\lambda_i C_{1i}}{1 - k_{11}(1-\beta)} \tag{61}$$

and summing Eqs. (60) and (61), we obtain:

$$\frac{N_{11}}{\ell_{11}} + \frac{N_{12}}{\ell_{12}} = \frac{k_{12}(1-\beta)\left(\frac{N_{21}}{\ell_{21}} + \frac{N_{22}}{\ell_{22}}\right) + k_{11}\sum_{i=1}^{D}\lambda_i C_{1i} + k_{12}\sum_{i=1}^{D}\lambda_i C_{2i}}{1 - k_{11}(1-\beta)}. \tag{62}$$

Using Eq. (62), we obtain:

$$\frac{dN_{21}}{dt} = \frac{k_{21}(1-\beta)k_{12}(1-\beta)}{1-k_{11}(1-\beta)}\left(\frac{N_{21}}{\ell_{21}} + \frac{N_{22}}{\ell_{22}}\right) - \frac{N_{21}}{\ell_{21}} + \frac{k_{21}}{1-k_{11}(1-\beta)}\sum_{i=1}^{D}\lambda_i C_{1i} + \frac{k_{12}(1-\beta)k_{21}}{1-k_{11}(1-\beta)}\sum_{i=1}^{D}\lambda_i C_{2i}. \tag{63}$$

We also have:

$$\frac{dN_{22}}{dt} = k_{22}(1-\beta)\left(\frac{N_{21}}{\ell_{21}} + \frac{N_{22}}{\ell_{22}}\right) - \frac{N_{22}}{\ell_{22}} + k_{22}\sum_{i=1}^{D}\lambda_i C_{2i}. \tag{64}$$

Using Eq. (62) we obtain:

$$\frac{dC_{1i}}{dt} = \frac{\beta_i k_{12}(1-\beta)}{1-k_{11}(1-\beta)}\left(\frac{N_{21}}{\ell_{21}} + \frac{N_{22}}{\ell_{22}}\right) + \frac{\beta_i k_{11}}{1-k_{11}(1-\beta)}\sum_{i=1}^{D}\lambda_i C_{1i} + \frac{\beta_i k_{12}}{1-k_{11}(1-\beta)}\sum_{i=1}^{D}\lambda_i C_{2i} - \lambda_i C_{1i}. \tag{65}$$

We also have:

$$\frac{dC_{2i}}{dt} = \beta_i\left(\frac{N_{21}}{\ell_{21}} + \frac{N_{22}}{\ell_{22}}\right) - \lambda_i C_{2i}. \tag{66}$$

Eqs. (63) through (66) form our reduced kinetics equations, along with the equations for N_{11}/ℓ_{11} and N_{12}/ℓ_{12} in Eqs. (60) and (61).

If we write the reduced set of equations ignoring delayed neutrons we obtain:

$$\frac{dN_{21}}{dt} = \left(\frac{k_{12}k_{21}}{\Delta_1} - 1\right)\frac{N_{21}}{\ell_{21}} + \frac{k_{12}k_{21}}{\Delta_1}\frac{N_{22}}{\ell_{22}} \tag{67}$$

$$\frac{dN_{22}}{dt} = k_{22}\frac{N_{21}}{\ell_{21}} - \Delta_2\frac{N_{22}}{\ell_{22}} \tag{68}$$

and where N_{11} and N_{12} are given by:

$$\frac{N_{11}}{\ell_{11}} = \frac{k_{11}k_{12}}{\Delta_1}\left(\frac{N_{21}}{\ell_{21}} + \frac{N_{22}}{\ell_{22}}\right) \tag{69}$$

$$\frac{N_{12}}{\ell_{12}} = k_{12}\left(\frac{N_{21}}{\ell_{21}} + \frac{N_{22}}{\ell_{22}}\right). \tag{70}$$

We now obtain the inhour equation for the reduced set of equations without delayed neutrons. We assume exponential solutions of the form $N_{jk}{}^0 e^{\omega t}$, substitute into Eqs. (67) and (68) and obtain from the condition that the determinant of the matrix of coefficients must vanish

$$\Delta_1(\Delta_2 + \omega\ell_{22})(1 + \omega\ell_{12}) = k_{12}k_{21}(1 + \omega\ell_{22}). \tag{71}$$

If we further assume that $\ell_{22} = \ell_{21} = \ell_S$, Eq. (71) reduces to:

$$\omega\ell_S = \frac{1}{\Delta_1}(k_{12}k_{21} - \Delta_1\Delta_2)$$

which along with Eq. (10) and the general relation

$\omega \approx \rho/\ell$ where ℓ is the effective prompt lifetime during the excursion yields

$$\ell \approx \ell_S \frac{\Delta_1}{\Delta_1 + \Delta_2}.$$

Therefore, the same relation that was obtained for the steady state is also approximately valid during an excursion as long as the system is below prompt fast critical.

REFERENCES

1. AECD-3645. *The Reactor Handbook*, Vol. 1, Physics, Chap. 1.6, p. 533.
2. R. Ehrlich and H. Hurwitz Jr., *Multigroup Methods for Neutron Diffusion Problems*, Nucleonics, Vol. 12, No. 2 (1954).
3. R. Avery, *Coupled Fast-Thermal Power Breeder*. Nuclear Sci. and Eng., Vol. 3, No. 2 (1958).
4. R. Avery *et al.*, *Coupled Fast-Thermal Power Breeder Critical Experiment*. P/2160, Vol. 12, these Proceedings.

APPENDIX B

Notes on the physics of neutronics coupling

M. Salvatores

1- Eigenvalues and flux tiltiness of the VCTR

The « decoupling » of spatial regions in a reactor is a well-recognized phenomenon that has been pointed out in the early reactor physics studies. The decoupling/coupling effects are physics effects that can be found in large reactors, where spatial regions can act as regions weakly or more strongly coupled but also in coupled reactors of the type of the VCTR. In case of a coupled system, the "flux tilting" between two regions, can be induced e.g. by the asymmetrical insertion of a perturbation (reactivity) in the system.

The potential flux tiltiness (and its impact on the time evolution of the power distributions) in the system can be associated to the so-called Boltzmann operator eigenvalue separation (see e.g. Refs. B.1-2) which is defined with the first and second eigenvalues as SVP = $\lambda_{B1}/(\lambda_{B1} - \lambda_{B2})$. λ_{B1} is better known as k_{eff}. Past studies have shown that a reactor will be less sensitive to asymmetrical perturbations if the SVP is small.

In the case of a coupled system, one can easily get the eigenvalues corresponding to the Avery matrix associated, e.g. to two coupled cores, as in the case of the VTR:

$$A = \begin{Bmatrix} k_{11} & k_{12} \\ k_{21} & k_{22} \end{Bmatrix}$$

Reminding that the eigenvalues for a square matrix A are given by Det $(A - \lambda_{Av} I_n) = 0$, one gets:

$$\lambda_{Av1} = \{[(k_{11})^2 + (k_{22})^2 - 2\times k_{11}\times k_{22} + 4\times k_{12}\times k_{21}]^{0.5} + k_{11} + k_{22}\}/2$$

$$\lambda_{Av2} = \{-[(k_{11})^2 + (k_{22})^2 - 2\times k_{11}\times k_{22} + 4\times k_{12}\times k_{21}]^{0.5} + k_{11} + k_{22}\}/2$$

For a "toy model" of a coupled system (defined by M. Aufiero from UCB as a sphere[1] with a fast and a thermal zone strongly coupled), the following parameters were found:

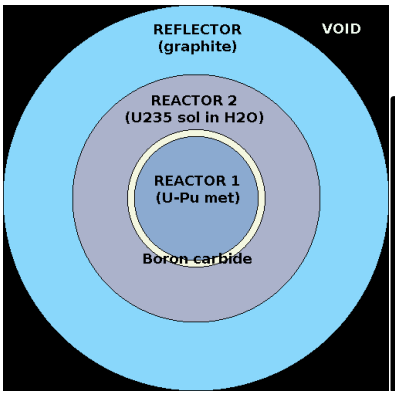

Parameter	SERPENT	
K_{eff} all system	1.00074	± 10 pcm (abs)
L_{eff} all system	1.83732E-05	± 0.1% (rel)
K_{11}	0.80023	± 25 pcm (abs)
K_{12}	0.07115	± 5 pcm (abs)
K_{21}	0.55199	± 20 pcm (abs)
K_{22}	0.80418	± 13 pcm (abs)
L_{11}	9.10896E-09	± 0.2 % (rel)
L_{12}	2.09716E-08	± 0.3 % (rel)
L_{21}	3.58647E-05	± 0.3 % (rel)
L_{22}	3.86979E-05	± 0.1 % (rel)

For this "toy model" the following eigenvalues are obtained from the Avery theory: λ_{Av1} = 1.00064 and λ_{Av2} = 0.60377. The first eigenvalue, λ_{Av1}, is very close to the k_{eff} the system (i.e. to λ_{B1}) calculated by SERPENT (respectively 1.00064 and 1.00074). The second eigenvalue for the "toy model", λ_{B2}, was also calculated by G. Palmiotti with the standard ERANOS procedure to get the eigenvalues of the corresponding Boltzmann operator. It was found that λ_{B2} = 0.63532, in good agreement with the value for λ_{Av2} given above (0.60377). The difference between the two eigenvalues is probably due to the ERANOS spatial and

[1] The central region ("fast reactor") consists in a 9 cm sphere of a (30%-70%) mixture of metallic ^{239}Pu and ^{238}U. The "thermal reactor" is made of a 9 cm thick spherical region of a water solution of ^{235}U (5.9 w%). The two regions are separated by a 1-cm thick boron carbide filter, to prevent the thermal neutrons from inducing fissions in the fast reactor. A graphite reflector surrounds the whole system.

energy discretization of the toy problem; further optimization of the ERANOS modeling options—not attempted here—would probably result in lower discrepancies.

This shows, as expected, that the eigenvalue "separation" calculated via the Avery theory is closely related to the coupled system Boltzmann operator eigenvalue separation and can be interpreted in physics terms as follows: cores tightly coupled (i.e. each characterized by a significant sub-criticality and with at least one significant coupling coefficient) show a large eigenvalue separation and, as a consequence, very small power shapes tiltiness. On the contrary, cores loosely coupled (i.e. each very close to criticality and with relatively small coupling coefficients), are expected to show significant power shape tiltiness. The following simple cases (from loosely, in principle large size, coupled cores to small, strongly coupled cores) illustrate the previous statement:

$k_{11} = k_{22} = 0.98$; $k_{12} = k_{21} = 0.02 \Rightarrow \lambda_{Av1} = 1$ and $\lambda_{Av2} = 0.96 \Rightarrow$ SVP = 25

$k_{11} = k_{22} = 0.95$; $k_{12} = k_{21} = 0.05 \Rightarrow \lambda_{Av1} = 1$ and $\lambda_{Av2} = 0.90 \Rightarrow$ SVP = 10

$k_{11} = k_{22} = 0.90$; $k_{12} = k_{21} = 0.10 \Rightarrow \lambda_{Av1} = 1$ and $\lambda_{Av2} = 0.80 \Rightarrow$ SVP = 5

$k_{11} = k_{22} = 0.80$; $k_{12} = k_{21} = 0.20 \Rightarrow \lambda_{Av1} = 1$ and $\lambda_{Av2} = 0.60 \Rightarrow$ SVP = 2.5

$k_{11} = k_{22} = 0.80$; $k_{12} = 0.5$; $k_{21} = 0.08 \Rightarrow \lambda_{Av1} = 1$ and $\lambda_{Av2} = 0.60 \Rightarrow$ SVP = 2.5

In summary, the previous discussion indicates that in strongly coupled cores of the type of VCTR, no strong power shape tiltiness should be found e.g. in the case of asymmetric reactivity insertions.

2- Share of reactivity between the two regions of the VCTR

In order to evaluate the share of reactivity between the two regions of the VCTR, one can use the Avery theory formulation:

$$\rho \approx \frac{\frac{1}{\Delta_1}}{\frac{1}{\Delta_1}+\frac{1}{\Delta_2}}\frac{\delta\nu_1}{\nu_1} + \frac{\frac{1}{\Delta_2}}{\frac{1}{\Delta_1}+\frac{1}{\Delta_2}}\frac{\delta\nu_2}{\nu_2}. \qquad (14)$$

We can generalize the above result to N coupled reactors and find that:

$$\rho \approx \sum_{i=1}^{N} \alpha_i \frac{\delta\nu_i}{\nu_i}, \qquad (15)$$

where

$$\alpha_i = \frac{1}{\Delta_i} \Big/ \sum_{j=1}^{N} \frac{1}{\Delta_j}. \qquad (16)$$

The previous considerations lead to the concept of division of reactivity. α_i, the fraction of reactivity in reactor i, is defined as the ratio of the over-all reactivity to $\delta\nu_i/\nu_i$, where the reactivity results from the change of ν_i to $\nu_i + \delta\nu_i$.

where the Δ_i are defined as $(1 - k_{ii})$.

The two alpha values give the reactivity share between them. This share is the best indicator for the coupled core optimization and control and should be systematically used in view of any safety analysis.

References

[B.1] D.C. Wade and R.A. Rydin, "Dynamics of Nuclear Systems" University of Arizona Press (1972)

[B.2] G.Palmiotti and M.Salvatores, Nucl. Sci. Eng. Vol. 87, p. 333-348 (1984)

APPENDIX C

Preliminary Coupled Reactor Deterministic Calculations Using MAMMOTH

J. Ortensi, F.N. Gleicher, M. DeHart

PROBLEM DESCRIPTION:

A single core design was selected for analysis and comparison against the Monte Carlo reference code Serpent. In this design there is a central core composed of hexagonal blocks with a total hexagonal span of 70 cm across and 100 cm tall. A central chamber with room for experiments occupies the middle of the core. The central core is surrounded by a reflector region followed by a second core region. The fuel blocks of the second core are hexagonal and have an approximate span of 8 cm and are 200 cm tall. A graphite reflector surrounds this second core region. A graphic of mid-plane slice of the reactor is shown in Figure B.1.

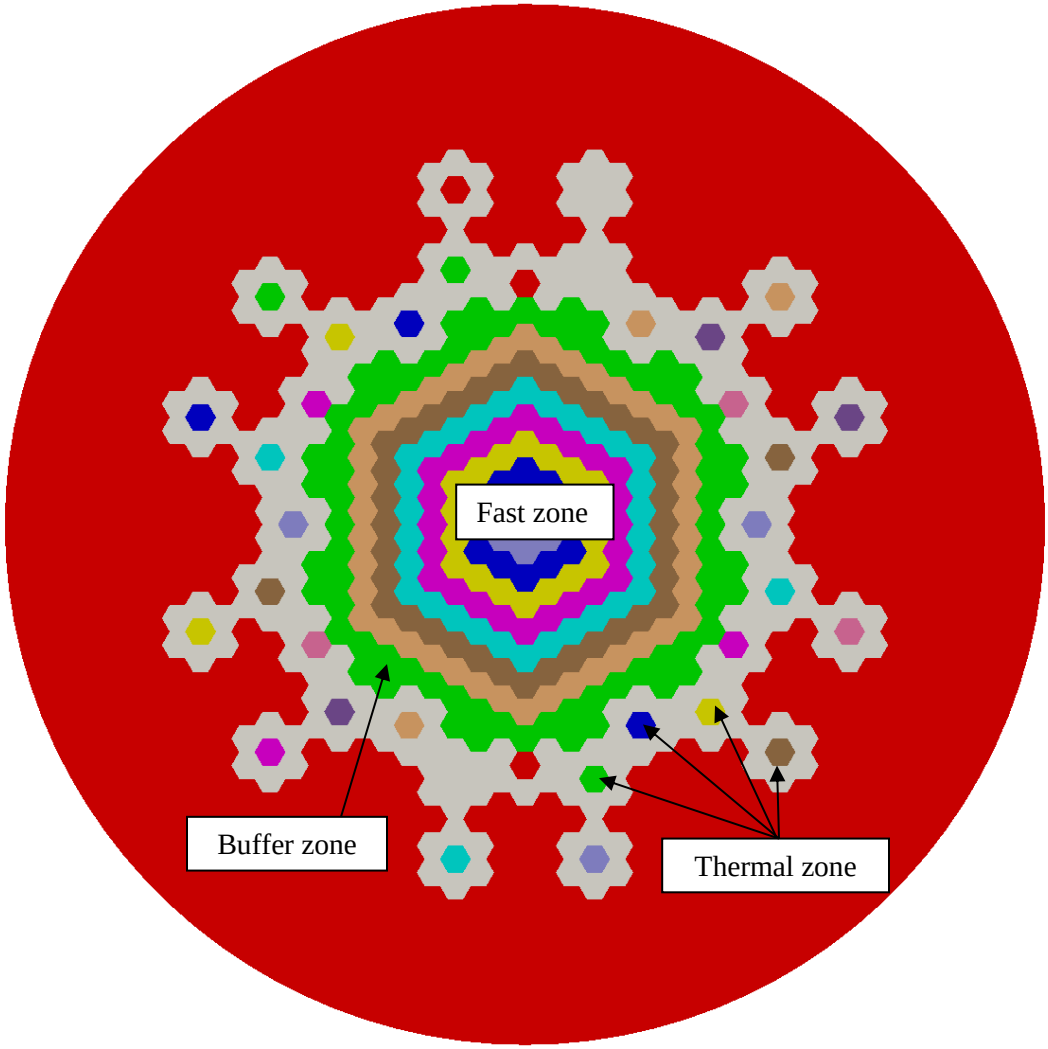

Figure B.1: Graphic of a horizontal slice (mid-plane) of the reactor.

The finite element model of the core is composed of homogenized hexagonal assemblies spatially discretized with six WEDGE6 elements. A view of the inner core with the subdivision of each hexagon region is shown in Figure B.2.

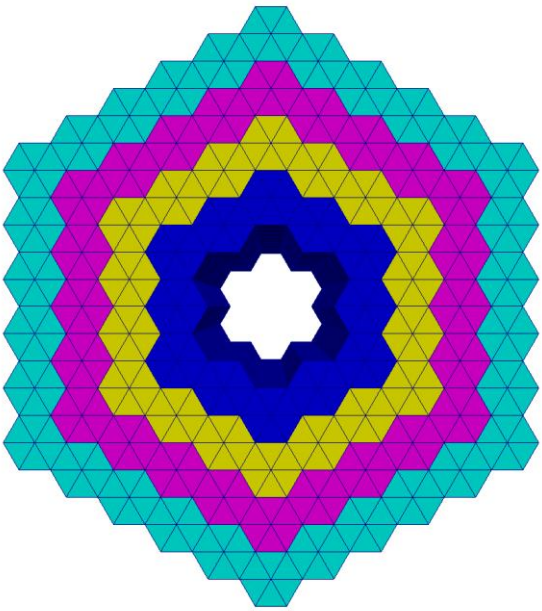

Figure B.2: Graphic of the central core section with spatial element discretization.

The wedges can be further subdivided by the MOOSE refinement system to give results that are more spatially resolved. A vertical slice of the reactor core is shown in Figure B.3 while a vertical slice of the inner core and experiment chamber are shown in Figure 4. The axial discretization is shown in Figure B.4.

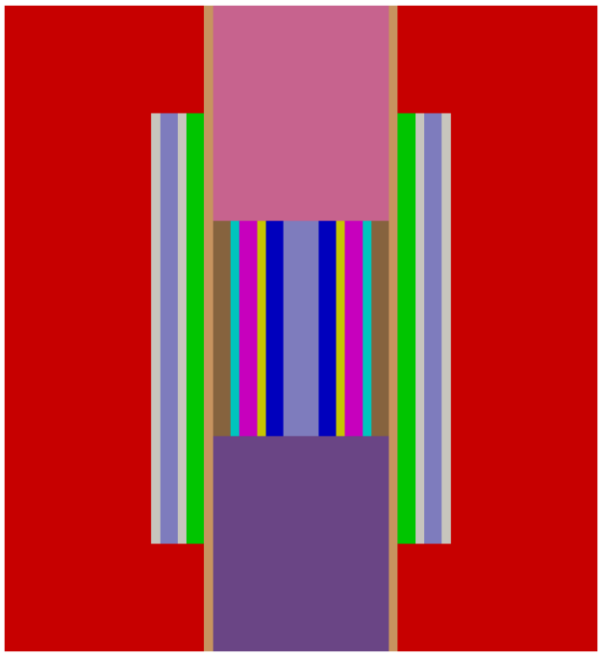

Figure B.3: Graphic of vertical slice (midplane) or reactor.

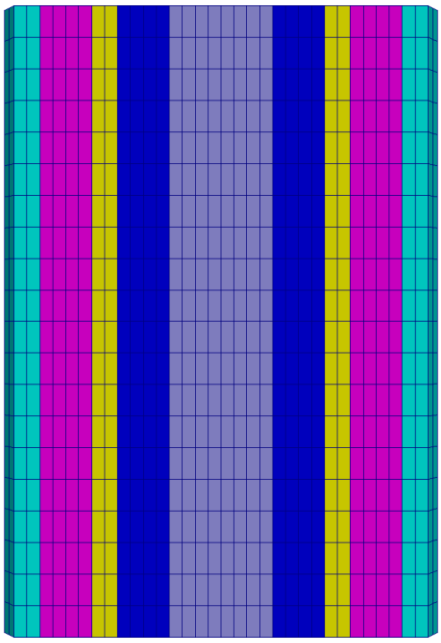

Figure B.4: Graphic of vertical slice (mid-plane) of inner core with axial discretization.

MULTI-GROUP CROSS SECTION GENERATION:

The multi-group cross sections used by MAMMOTH were generated with the same 3D Serpent-2 model used to generate the reference k-eff and power distribution. A different set of multi-group cross sections was generated for each Serpent "Universe", i.e. for each colored zone of Figure B.1. Three energy group structures were also considered: 35, 21 and 11 groups (see Table B.I). At this point, no attempts were made to optimize neither the energy group structure nor the spatial distribution of the cross section sets.

The Serpent runtimes and the uncertainties in the P1 scattering matrix are dependent on the number of particles and active cycles. The full core geometry is applied to prepare all of the cross sections with a single run, which took 46.6 minutes with 120 CPUs (Intel(R) Xeon(R) CPU E5-2680 v3 @ 2.50GHz). The model in Serpent was run with one million particles per cycle with 2000 active and 100 inactive cycles. The P0 scattering matrix uncertainty for **fast** diagonal terms is less than 1% and for **fast** off-diagonal terms (~1E-3 magnitude) is less than 4%. The P1 scattering matrix uncertainty for **fast** diagonal terms is less than 2% and for the **fast** off-diagonal terms (~1E-3 magnitude) is less than 10%. These statistical uncertainties can be further reduced by increasing the number of particles per cycle or the number of cycles used in the Monte Carlo simulations.

In addition, Serpent uses the out-scattering correction of the transport cross section with standard tallies to compute the total and group transfer cross sections but tallying the incident and emergent directional vectors of the neutrons undergoing scattering reactions to obtain the average scattering cosine.

Table B.I: 35, 21 and 11 energy group structures (lower bound in eV)

Group number	35-group structure	21-group structure	11-group structure
1	1.00E+07	6.07E+06	2.23E+06
2	6.07E+06	2.23E+06	3.02E+05
3	3.68E+06	8.21E+05	4.09E+04
4	2.23E+06	3.02E+05	9.12E+03
5	1.35E+06	1.11E+05	1.23E+03
6	8.21E+05	4.09E+04	1.49E+02
7	4.98E+05	1.50E+04	2.26E+01
8	3.02E+05	9.12E+03	4.00E+00
9	1.83E+05	3.35E+03	2.80E-01
10	1.11E+05	1.23E+03	5.80E-02
11	6.74E+04	4.54E+02	0.00E+00
12	4.09E+04	1.49E+02	-
13	2.48E+04	6.79E+01	-
14	1.50E+04	2.26E+01	-
15	9.12E+03	8.32E+00	-
16	5.53E+03	4.00E+00	-
17	3.35E+03	6.25E-01	-
18	2.03E+03	2.80E-01	-
19	1.23E+03	1.40E-01	-
20	7.49E+02	5.80E-02	-
21	4.54E+02	0.00E+00	-
22	3.04E+02	-	-
23	1.49E+02	-	-
24	9.17E+01	-	-
25	6.79E+01	-	-
26	4.02E+01	-	-
27	2.26E+01	-	-
28	1.37E+01	-	-
29	8.32E+00	-	-
30	4.00E+00	-	-
31	6.25E-01	-	-
32	2.80E-01	-	-
33	1.40E-01	-	-
34	5.80E-02	-	-
35	0.00E+00	-	-

RESULTS:

Currently, the total heating power is applied in the calculation of the power distribution. This total heating power includes all heat generated in the system. Serpent uses an approximation based on the total fission rate and empirical heating values directly proportional to fission energy. For example, the heating value for U-235 fission is 202.27 MeV and the values for other nuclides are scaled according to the ratios of fission Q-values. This energy deposition can be further improved in the future by explicitly determining the two dominant components: 1) the local energy deposition from fission fragments and 2) the gamma heating (with a Rattlesnake gamma transport simulation).

The fraction of the power produced in the inner and outer core, and the core eigenvalue are given in Table B.II for different energy group structures and angular discretizations. The inner core is labeled as "Fast Zone" and the outer core is labeled as "Thermal Zone." The results presented in the first row were generated with Serpent whereas the other results were generated with Rattlesnake. Run times were, respectively, about 1 minute and 5 minutes for the 11- and 35-group diffusion calculations using a typical number of processors readily available to analysts on the HPC. S_N transport calculations ran longer than expected because of issues encountered with the acceleration method (NDA) and the P_N is currently not accelerated. These deficiencies can and will be resolved. For example, the run time for the 11-group S4 calculation was about 30 minutes using the same number of processors as for the diffusion calculations. A properly operating acceleration scheme will decrease the run time by a factor that still needs to be determined, but typically a factor of 10. The scattering order was the same for the S4, S8 and P3 calculations (P1).

Table B.II: A list of the Method, the fast and thermal power produced in each zone, the core eigenvalue and the total time for each steady state eigenvalue solve.

Method	Fast Zone	Thermal Zone	Eigenvalue
Serpent	0.4070	0.5930	1.00817
11 G Diffusion	0.3916	0.6084	1.01527
21 G Diffusion	0.3915	0.6085	1.00925
35 G Diffusion	0.3918	0.6082	1.00746
11 G S4	0.4079	0.5921	1.02798
21 G S4	0.4073	0.5927	1.02281
35 G S4	0.4069	0.5931	1.02109
11 G S8	0.4079	0.5921	1.02804
21 G S8	0.4072	0.5928	1.02289
35 G S8	0.4067	0.5933	1.02116
11 G P3	0.4082	0.5918	1.02710
21 G P3	0.4077	0.5923	1.02184
35 G P3	0.4074	0.5926	1.02009

For this selected core design, there is cancellation of errors in the diffusion solution, and thus the core eigenvalue appears very close to the reference Serpent Monte Carlo solution (+70 pcm for the 35-group calculation). The transport methods all produce core eigenvalues that are larger than the reference solution by 1200 to 2000 pcm. The model overestimates the reference solution potentially due to insufficient cross section resolution in the reflector. Note that a single cross section set is used in the graphite reflector, a region with significant spectral changes. Even though the cross sections for graphite are pretty flat over the fast and epithermal energy ranges, the 1/v region might require separate cross sections in the various reflector regions. A simple spectral analysis should provide enough information to significantly improve the solutions.

A comparison of the assembly by assembly power distributions shows that the diffusion calculations are roughly within + 6% and -5% of the reference Serpent calculations. The S4 and S8 calculations are roughly

within + 2% and -1% of the reference Serpent calculations. The P3 calculations are also roughly within + 2% and -1% of the reference Serpent calculations.

The implementation of the SPH method in MAMMOTH opens the possibility of generating corrected cross section tabulations that preserve the Monte Carlo reaction rates with few groups and a coarse spatial discretization. This could lead to faster run times and the much-improved results, which have been observed during the analysis of the Transient Test Reactor facility (TREAT).

CONCLUSIONS:

As requested by the project, a rapid initial assessment of a coupled thermal/fast core was performed by the MAMMOTH tools set and compared to Serpent. For eigenvalues, the 3D diffusion solution generated by Rattlesnake can be as close as 70 pcm to the reference value with only a relatively limited number of energy groups (11 to 35); however, this accuracy is due to cancellation of errors. For the diffusion solutions, differences in the integrated whole assembly power are between + 6% and -5% to the reference Serpent calculations. Running times were, respectively, about 1 minute and 5 minutes for the 11- and 35-group diffusion calculations using a typical number of processors readily available to analysts on the HPC. The S4, S8 and P3 eigenvalues, are higher than the reference value by +1200 pcm to +2000 pcm; however, compared to diffusion, the agreement with Serpent is improved for the power distribution (between + 2% and -1%). These results are encouraging and could probably be improved through optimization of the various options available to the analysts. Even though more work is still required, these preliminary results also seem to indicate that diffusion calculations using a relatively limited number of energy groups are sufficient to capture the change in the neutron spectrum happening between the fast and thermal zone—if the multi-group cross sections are generated appropriately. If deemed necessary by the project, the MAMMOTH model could be refined and used for 3D transient analyses.